

**Therapeutic Wnt/ $\beta$ -catenin signaling  
activation and regulation for lung repair  
in chronic obstructive pulmonary disease**



Rita Ribeiro da Silva Alves da Costa

PhD thesis

Munich, 2020



From the Lung Repair and Regeneration Research Unit (LRR)

Director: Prof. Dr. Melanie Königshoff

Therapeutic Wnt/ $\beta$ -catenin signaling  
activation and regulation for lung repair in  
chronic obstructive pulmonary disease



Thesis for the attainment of the degree of

Doctor of Philosophy (Ph.D.)

at the Faculty of Medicine, Ludwig-Maximilians University Munich

by

Rita Ribeiro da Silva Alves da Costa

from Porto, Portugal

Munich, 2020





With the approval of the Faculty of Medicine of the Ludwig-Maximilians University  
Munich

Evaluators:

Supervisor: Prof. Dr. Melanie Königshoff

Second expert: Dr. Kamyar Hadian

Dean: Prof. Dr. med. dent. Reinhard HICKEL

Date of oral defense: 5<sup>th</sup> of November, 2020



I dedicate this thesis to my loving daughter Benedita.

*Minha adoração, meu doce mais lindo, amo-te muito,*

*Mamã.*



# Table of contents

Table of contents .....	I
List of abbreviations and symbols.....	III
Summary .....	V
1. Introduction .....	1
1.1. Chronic obstructive pulmonary disease.....	2
1.1.1. Epidemiology of COPD .....	4
1.1.2. Pathology, pathogenesis and pathophysiology of COPD.....	8
1.1.3. Treatment of COPD .....	10
1.2. Wnt signaling.....	11
1.2.1. Wnt signaling in lung development, injury and repair .....	13
1.2.2. Wnt signaling in COPD.....	15
1.2.3. Wnt signaling modulation .....	16
2. Hypothesis and aims .....	19
3. Materials and methods .....	21
3.1. Cell culture .....	21
3.2. Reagents.....	22
3.3. High-throughput small compound screen.....	22
3.4. Drug selection .....	23
3.5. Luciferase reporter assay .....	24
3.6. Cell viability assay .....	25
3.7. Animals.....	25
3.8. Mouse lung epithelial cell isolation .....	26
3.9. Murine lung organoid culture .....	27
3.10. Organoid quantification.....	28
3.11. Immunofluorescence .....	28
3.12. Amlexanox preparation and <i>in vivo</i> administration .....	29

3.13. Elastase mouse model of emphysema .....	29
3.14. Lung function measurement .....	30
3.15. Blinding .....	30
3.16. RNA extraction, cDNA synthesis and quantitative real-time PCR.....	31
3.17. Statistical analysis .....	33
4. Results .....	35
4.1. Wnt/ $\beta$ -catenin luciferase reporter cell based screening identifies human approved drugs as Wnt activators .....	35
4.2. Inhibition of $\beta$ -catenin reduces Wnt dependent luciferase activity in amlexanox and phenazopyridine hydrochloride treated cells .....	41
4.3. Amlexanox and phenazopyridine hydrochloride induce primary adult epithelial cell derived organoid formation.....	43
4.4. Inhibition of $\beta$ -catenin reduces amlexanox and phenazopyridine hydrochloride organoid formation capacity .....	48
4.5. Amlexanox treatment improves lung function and induces Wnt related genes while reducing disease markers in a mouse model of lung emphysema .....	49
5. Discussion.....	53
6. Conclusion and future directions .....	57
7. References .....	59
Appendix.....	i
Acknowledgments.....	iii
List of scientific publications.....	v
<i>Affidavit</i> .....	vii
Confirmation of congruency .....	ix

## List of abbreviations and symbols

.	decimal separator
<	less than
°C	degree Celsius
µl	microliters
µm	micrometers
AAT	alpha-1 antitrypsin
AATD	alpha-1 antitrypsin deficiency
ACT	acetylated tubulin
cDNA	complementary deoxyribonucleic acid
CO <sub>2</sub>	carbon dioxide
COPD	chronic obstructive pulmonary disease
Ct	cycle threshold
DMEM	Dulbecco's Modified Eagle's Medium
DMSO	dimethyl sulfoxide
DNA	deoxyribonucleic acid
EGF	epidermal growth factor
EMA	European Medicine Agency
et al.	and others
FBS	fetal bovine serum
FDA	Food and Drug Administration
FEV <sub>1</sub>	forced expiratory volume in one second
Fgf	fibroblast growth factor
FVC	forced vital capacity
g	g-force
GARD	Global Alliance against Chronic Respiratory Diseases
GO	gene ontology
GOLD	Global Initiative for Chronic Obstructive Lung Disease
h	hours
HCl	hydrochloride
HEPES	4-(2-hydroxyethyl)-1-piperazineethanesulfonic acid
Hprt	hypoxanthine-guanine phosphoribosyltransferase
kg	kilograms

LEF	lymphoid enhancer factor
LiCl	lithium chloride
M	molar
mg	milligrams
min.	minutes
ml	milliliters
mm	millimeters
mM	millimolar
MMP	metalloproteinase
mRNA	messenger ribonucleic acid
NCD	non-communicable disease
NIH	National Institutes of Health
NKD	naked cuticle
p	probability value
PBS	phosphate buffered saline
PCLS	precision cut lung slices
PCR	polymerase chain reaction
PET	polyester
pH	power of hydrogen
PS	polystyrene
qPCR	quantitative real-time polymerase chain reaction
RNA	ribonucleic acid
s.	seconds
s <sup>-1</sup>	frequency
SD	standard deviation
SFTPC	surfactant protein C
SW	signal window
TCF	T-cell factor
U	units
WHO	World Health Organization
Wnt	wingless/int1
β	beta
Δ	delta



## Summary

Chronic obstructive pulmonary disease (COPD) is an incurable lung disease in which functional lung tissue, important for gas exchange, is lost (emphysema). Wnt/ $\beta$ -catenin signaling, crucial during lung repair, is reduced in COPD and pharmacological activation of the pathway *in vivo* as well as in *ex vivo* preclinical models, attenuates disease markers. The aim of this study was to identify a safe pharmaceutical compound able to activate Wnt/ $\beta$ -catenin signaling and assess its potential to induce lung repair in emphysema.

We screened 1216 FDA-approved chemicals for Wnt/ $\beta$ -catenin signaling activation, using a cell-based Wnt reporter luciferase system. We further studied the regeneration potential of the approved drugs using a murine adult epithelial cell derived lung organoid assay and an *in vivo* model of lung emphysema.

With the drug screen and further confirmatory assays we identify amlexanox as a new FDA-approved compound which can activate Wnt/ $\beta$ -catenin signaling. Using murine primary adult epithelial cell derived lung organoids, we show that amlexanox is able to initiate lung repair, demonstrated by increases in organoid formation capacity. In both cases the treatment effect could be reversed by pharmacological Wnt inhibition, confirming the Wnt-dependent mechanism of action of amlexanox. *In vivo*, mouse lung function, measured by dynamic compliance, was improved after 7 days of 50 mg/kg amlexanox administration. Gene expression analysis of important alveolar repair as well as disease markers, fibroblast growth factor 7 (*Fgf7*), hepatocyte growth factor (*Hgf*), ADAM metallopeptidase with thrombospondin type 1 motif 4 (*Adamts4*) and elastin (*El*n), indicated a pro-regenerative phenotype in mouse lungs which received amlexanox

treatment. These data indicate that amlexanox may be useful for the regenerative treatment of COPD.

---

## 1. Introduction

Chronic diseases, also defined as non-communicable diseases (NCDs), are the leading cause of ill health in the world, likely to be of long duration and responsible for 71% of global and 80% of premature deaths (Bennett et al., 2018). The four major NCDs are cardiovascular diseases, cancers, diabetes and chronic obstructive pulmonary disease (COPD).

In 2011, United Nations countries agreed on nine global NCDs targets across a range of risk factors linked to lifestyle and demographic changes, such as tobacco use, physical inactivity, excessive alcohol consumption, unhealthy diets and air pollution. The World Health Organization (WHO) developed a Global Action plan to be implemented at high coverage levels with the aim of reducing NCDs burden and securing sustainable development in all countries. Ultimately, for reducing mortality from NCDs novel strategies for prevention, early detection and effective treatment options are needed (Heller et al., 2019).

In parallel, the Global Alliance against Chronic Respiratory Diseases (GARD), an alliance of volunteer organizations, institutions and agencies, works globally towards improving lung health, acting according to local needs, both in disease prevention and control (Bousquet, Dahl & Khaltayev, 2007).

Chronic lung diseases include asthma, pulmonary hypertension, occupational lung diseases, respiratory allergies, and COPD, and are the major responsible causes of reduced or early lung function decline in the world population (Figure 1.1.).

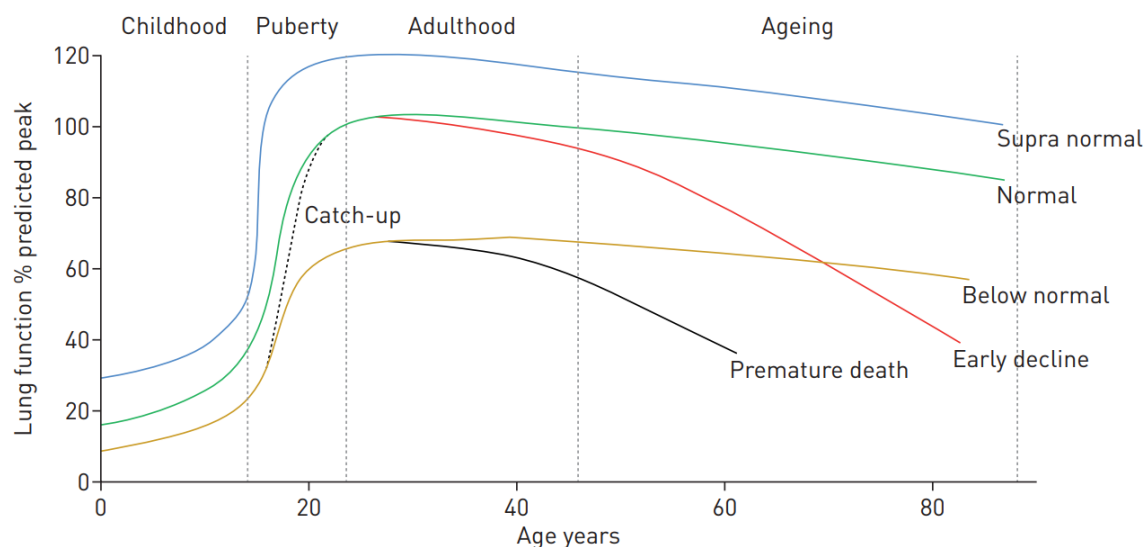


**Figure 1.1.** Different predicted lung function trajectories through the human life (Agusti & Faner, 2019; Agusti et al., 2019). In all trajectories there are three main phases: growth phase, where the lung is still under development, plateau phase, corresponding to the early adulthood, and decline phase, associated with lung ageing. “Catch-up” refers to evidenced recovery cases. Schematic adapted from the Fletcher-Peto diagram (Fletcher & Peto, 1977).

2

The focus of this thesis is the development of effective therapies for COPD, using relevant preclinical disease models and targeting underlying mechanisms of aberrant lung tissue repair, namely dysregulated Wnt/ $\beta$ -catenin signaling.

### 1.1. Chronic obstructive pulmonary disease

Chronic obstructive pulmonary disease (COPD) was considered for a long time a single self-inflicted lung disease, caused by tobacco smoking, characterized by an inflammatory response damaging the airways (Figure 1.2.) (Agusti & Hogg, 2019).

Current knowledge of COPD considers it a result of multiple long-term, dynamic, and cumulative gene–environment interactions, which shape the development, maintenance, and function of the lung, as well as of other organs, through complex biologic mechanisms, including but not restricted to inflammation. Thus, COPD is

a clinical syndrome which manifests as a heterogeneous lung disease, comprising various disorders of different origins, resulting in a partly reversible airflow limitation to which there is no curative treatment (Celli & Wedzicha, 2019).

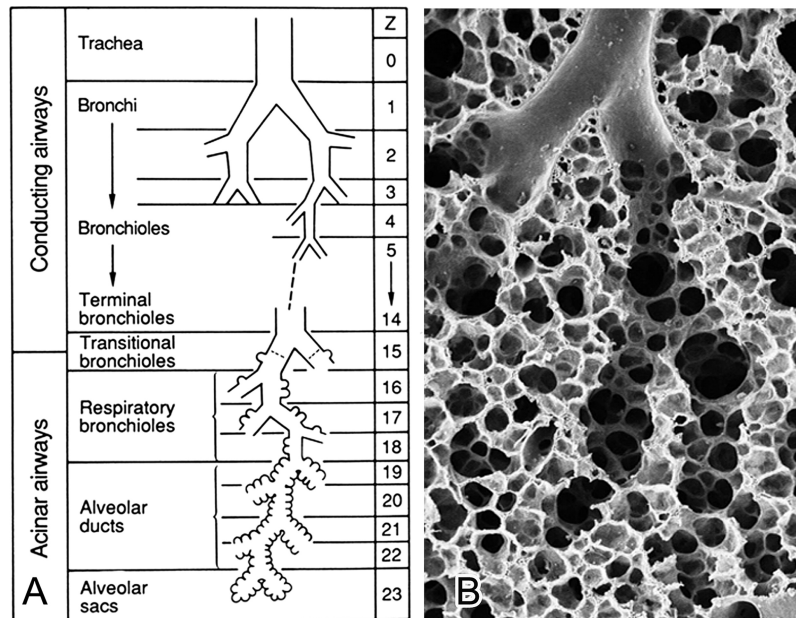


**Figure 1.2.** Human airway tree. **A)** scheme of the hierarchy of the airways divided into conducting airways and acinar or respiratory airways where gas exchange occur and **B)** scanning electron micrograph of a human section of the lung showing the characteristic fractal geometry which allows increased surface area for gas exchange within a confined space (Weibel, 2013).

COPD is characterized by chronic respiratory symptoms, caused by structural pulmonary abnormalities, such as airways disease or emphysema (the destruction of alveolar airspaces) leading to lung function impairment (Celli & Wedzicha, 2019).

Importantly, the understanding of COPD over the past decades has improved significantly. Each year, more people die with COPD, rather than from COPD (Collaborators, 2020). Despite this fact, there are many challenges in clinical

practice involving prevention, early diagnosis and treatment of COPD that need to be met (Agusti, 2019).

In 1997, the Global Initiative for Chronic Obstructive Pulmonary Disease (GOLD) was founded to raise awareness of COPD and improve both disease prevention and treatment. In 2001, the GOLD organization established a classification for the diagnosis of COPD, in order to divide patients into different categories according to airflow limitation severity. This classification is since then the basis for diagnosis and considers the ratio of two measurements obtained on pulmonary function test (spirometry). One is the patient's forced expiratory volume in one second ( $FEV_1$ ), which measures the air volume a person can first exhale after a forced breath during the first second. The second is the forced vital capacity (FVC), the total volume of air exhaled after a full inspiration (Rodriguez-Roisin et al., 2017). COPD is diagnosed when the ratio  $FEV_1/FVC$  is less than 0,70.  $FEV_1$  is reduced in COPD due to air trapping, thus the ratio  $FEV_1/FVC$  is also reduced.

As patients struggle for breath, COPD has a significant impact on the quality of life. This creates a great burden socially and economically, for the population who suffers from COPD, health care providers and governments (Quaderi & Hurst, 2018).

### **1.1.1. Epidemiology of COPD**

Since 2016, COPD is the third leading cause of death worldwide, being the top cause of death among respiratory diseases (Figure 1.3.). More than 3 million people died of COPD in 2015, accounting for 5% of all deaths in the world. This

---

number is estimated to increase to 6,9% by 2060 (World Health Organization 2018).

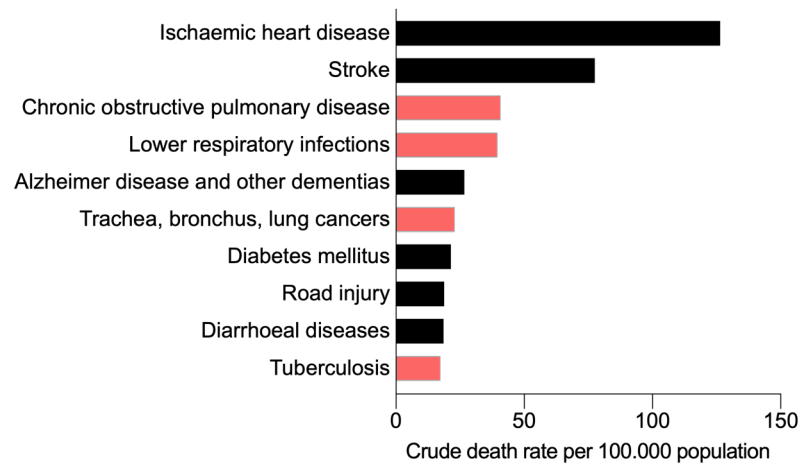


**Figure 1.3.** Top 10 global causes of death. Respiratory diseases are highlighted in red. Data retrieved from official numbers provided by the World Health Organization (WHO, 2018).

Although the number of COPD deaths has been either increasing or stabilizing, COPD mortality rates are declining in the majority of countries. On one hand due to improvements in COPD management, and on the other hand due to population growth and ageing (Lortet-Tieulent, Soerjomataram, Lopez-Campos, Ancochea, Coebergh & Soriano, 2019). COPD world prevalence is of 251 million cases (World Health Organization 2018). In the Rotterdam Study, a prospective cohort study encompassing 14926 participants ongoing since 1990, the overall incidence rate was approximately 9/1000 person-years (Terzikhan, Verhamme, Hofman, Stricker, Brusselle & Lahousse, 2016).

The main risk factors of COPD are tobacco smoke and age, but also include other airborne particle exposures, genetic susceptibility, gender, history of respiratory

infections, socioeconomic status, comorbidities, clinical history during lung growth and development (GOLD, 2019).

Tobacco smoke is the biggest risk factor of COPD in high- and middle-income countries. Meanwhile in low-income countries the main risk factor for COPD is exposure to indoor air pollution, such as the use of biomass fuels for cooking and heating (World Health Organization 2018). Furthermore, occupational exposures and outdoor air pollution also contribute to the pathogenesis of COPD.

The observations that only a proportion of individuals smoking develop COPD, and that around 25% of COPD patients never smoked, supports that genetic as well as epigenetic factors have an impact in disease onset (Kohansal, Martinez-Cambor, Agusti, Buist, Mannino & Soriano, 2009; Salvi & Barnes, 2009).

6 Hereditary deficiency of alpha-1 antitrypsin (AAT) is the major genetic susceptibility risk for COPD. Individuals with severe AAT deficiency (AATD) have an earlier onset of COPD, when compared to other patients, which often appears to not correspond to individual smoking history (Cazzola, Stolz, Rogliani & Matera, 2020). AAT is a protein encoded by the gene *SERPINA1* in humans, responsible for anti-protease activity. The protein targets include elastase, produced mainly by neutrophils, but also plasmin, thrombin, trypsin, chymotrypsin and plasminogen activator (Cohen, 1975). AAT is mainly synthesized in the liver, within the hepatocytes, in the intestine, pulmonary alveolar cells, neutrophils, macrophages, and cornea and is the most prevalent protease inhibitor in the human serum (Fagerberg et al., 2014; Strnad, McElvaney & Lomas, 2020). While proteases play important roles in the body, such as modulation of inflammation caused by host and microbial factors, their dysregulated and prolonged activity adversely impacts



---

tissue homeostasis. The existence of efficient endogenous control mechanisms able to dampen excessive protease activity is essential for the resolution of inflammation. Although AAT has a broad-spectrum of anti-inflammatory, immunomodulatory, anti-infective and tissue-repair action, its main function is to protect sensitive lung tissue from proteolytic damage (Jonigk et al., 2013). AATD is an autosomal co-dominant condition, predisposing for the development of different disease phenotypes, depending on whether they occur due to a deficient variant, with impaired activity, or lack of protein production (null alleles). Persons with normal circulating levels of AAT carry two copies of the wild-type M allele of *SERPINA1*. Point mutations can lead to two phenotypic scenarios: a toxic “gain of function”, due to retention of AAT in the liver, causing liver disease, or a “loss of function”, responsible for lack of circulating proteinase inhibitor, predisposing to early-onset of emphysema. In 95% of the severe cases, AAT deficiency results from a homozygous substitution of a single amino acid, Glu342Lys, encoded by the allele Z. The most common allele causing mild AATD, the S allele, encodes an amino acid replacement, Glu264Val. Patients carrying loss of function alleles, or having the genotypic combinations ZZ, ZNull, or NullNull need periodic monitoring as they are at bigger risk of developing lung emphysema. Heterozygotes patients with the MZ and SZ genotypes who smoke need to be closely monitored, since they have a significant increased risk, as compared with general MM allele carriers, of developing lung disease (Strnad, McElvaney & Lomas, 2020).

In a genome-wide association study, 279 genetic variants were associated with lung function signals. New signals implicating integrin subunit alpha V (ITGAV) and growth differentiation factor 5 (GDF5), as well as transforming growth factor beta 2 (TGFB2) and microfibrillar-associated protein 2 (MFAP2), provided new genetic

support for the importance of elastic fiber pathways in COPD, which are known to be aberrant or diminished in patients with lung emphysema (Shrine et al., 2019).

In an epigenome-wide association study, 28 differentially methylated sites associated with respiratory function and COPD. Functional analysis of the differentially methylated genes showed these were involved in alternative splicing, JAK-STAT signaling and axon guidance. Methylation status of 7 genes: suppressor of cytokine signaling 3 (SOCS3), strawberry notch homolog 2 (SBNO2), ral guanine nucleotide dissociation stimulator (RALGDS), islet cell autoantigen 1 (ICA1), mitotic deacetylase associated SANT domain protein (ELMSAN1), ATP binding cassette subfamily A member 1 (ABCA1) and jade family PHD finger 1 (JADE1); provided discriminatory power for COPD prediction (Bermingham et al., 2019). Of note, JADE1 has been described to inhibit Wnt/ $\beta$ -catenin signaling, through ubiquitylation of both phosphorylated and non-phosphorylated  $\beta$ -catenin (Chitalia et al., 2008).

### **1.1.2. Pathology, pathogenesis and pathophysiology of COPD**

COPD includes patients with widely varying clinical phenotypes and pathogenic mechanisms, which evolve according to different natural and individual histories (Agusti & Faner, 2018). Generally, the main pathological changes of COPD occur in the airways, lung parenchyma (the collection of small structures that pack an enormous surface area for gas exchange) and in the pulmonary vasculature (Suki, Stamenovic & Hubmayr, 2011). In turn, these are a consequence of a misbalanced proteolytic as well as anti-proteolytic activity, increased inflammatory response, and oxidative stress, increasing the amount of apoptotic and senescent cells and

decreasing cell proliferation and repair (Hadzic, Wu, Avdeev, Weissmann, Schermuly & Kosanovic, 2020) (Figure 1.4.).

The epithelium is the first responder to environmental stimuli. Changes in the epithelial cell layer occur by an initial stimuli and further aggravate through a spiral of complications (Randell, 2006). Toxic gases and particles induce tissue damage either by increasing oxidative stress, or by initiating an inflammatory response. Airflow limitation in COPD is due to airway remodeling, wall thickness, and mucous production as a result of the infiltration of immune cells, such as neutrophils, macrophages, and lymphocytes, in the lung tissue. An immune response to either foreign antigens (such as commensal organisms or pathogens) or self-antigens (such as elastin), can contribute to the pathogenesis and aggravation of COPD (Wen, Krauss-Etschmann, Petersen & Yu, 2018). Progressive narrowing, and destruction of terminal airways is followed by microvascular abnormalities which contribute to emphysema, the degradation of matrix proteins in the distal parts of the lung (Higham, Quinn, Cancado & Singh, 2019).

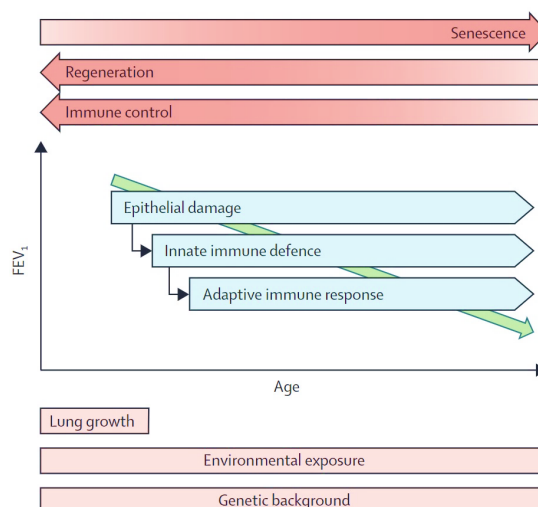


**Figure 1.4.** Summary of mechanisms involved in the pathogenesis of COPD (Decramer, Janssens & Miravitlles, 2012).

### 1.1.3. Treatment of COPD

As previously described, COPD is both a complex and heterogeneous disease. Complex because many components of the disease have no linear dynamic interactions, and heterogeneous because not every component is present in all patients, at all stages (Agusti, 2014).

In general, the main goals of current available therapies for COPD are limited to reducing symptoms and risk of disease progression (GOLD, 2019). Targets for pharmacological treatments include airway smooth muscle contraction, inflammation, mucus production, alpha-1-antitrypsin deficiency and respiratory infection (Kerstjens, Upham & Yang, 2019). The classes of drugs used for the treatment of COPD include bronchodilators, anti-inflammatory, anti-infective and mucoregulator agents (Singh et al., 2019).

10

---

To facilitate pharmacological management, the GOLD guidelines from 2017 introduced a new refined strategy recommending an ABCD assessment for patient grouping based on symptoms and exacerbation risk (Rodriguez-Roisin et al., 2017). Thus, pharmacological therapy of COPD is a patient-specific approach, individualized according to patient's symptoms, airflow limitation, exacerbations and tolerance to therapy's side effects. Bronchodilators target airway smooth muscle cells, allowing the airways to relax and become larger, improving patients breathing. The three major types of bronchodilators are:  $\beta_2$ -agonists, anticholinergics and xanthines. Within  $\beta_2$ -agonists and anticholinergics there are still two different classes based on their effect duration: short-acting (SABA and SAMA) and long-acting bronchodilators (LABA and LAMA) (Meek, Lareau, Fahy & Austegard, 2019). The different bronchodilators can be used alone or in

---

combination. Anti-inflammatory drugs aim at reducing inflammation, preventing and treating exacerbations. These include corticosteroids and phosphodiesterase-4 (PDE-4) inhibitors. Inhaled corticosteroids (ICS) are more commonly used in combination with a bronchodilator and treatment benefit can be measured by neutrophil blood count. For patients with prior history of hospitalization for an acute exacerbation, PDE-4 inhibitors have greater beneficial effects. Anti-infective agents such as vaccines, macrolides and antibiotics reduce the frequency of COPD exacerbations either through infection prevention or via immune system modulation. Finally, mucoregulators promote drainage of mucus from the lungs, reduce exacerbations and improve health status.

Lung transplantation is the only curative treatment option for patients with COPD. However, organ availability, patient's eligibility (such as advanced age or presence of other significant comorbidities), as well as tissue rejection and other associated complications make lung transplantation an unreliable treatment for most cases (Siddiqui & Diamond, 2018). Other surgeries which aim at lung volume reduction (LVRS), or removal of damaged tissue (e.g. bullectomy), are effective, but for a restricted number of patients and for short-term (Martinez & Chang, 2005; Meek, Lareau, Fahy & Austergard, 2019).

## **1.2. Wnt signaling**

Wnt signaling is crucial for cell proliferation, differentiation and migration, but also important during organ development, maintenance, injury, aging processes and diseases (Clevers & Nusse, 2012).

Wnts are a family of secreted glycoproteins which mediate cell to cell communication, either acting on neighboring cells or across a short distance (Skronska-Wasek, Gosens, Konigshoff & Baarsma, 2018; Wiese, Nusse & van Amerongen, 2018; Yeganeh et al., 2013). Wnt proteins are highly hydrophobic and show limited diffusion in the aqueous extracellular environment. Wnts regulate different signaling pathways which can be divided by  $\beta$ -catenin or  $\beta$ -catenin independent (Figure 1.5.). Focusing on the first signaling pathway,  $\beta$ -catenin is a transcriptional co-activator downstream effector of Wnt signalling in activated cells. In the absence of Wnts, the destruction complex formed by Axin, adenomatous polyposis coli (APC), glycogen synthase kinase-3 (GSK-3 $\beta$ ) and casein kinase 1 (CK1), is allocated in the cytoplasm, where it binds, phosphorylates, and ubiquitinates  $\beta$ -catenin through the E3-ubiquitin ligase  $\beta$ -TrCP before proteosomal degradation. In the presence of Wnts, these bind to Frizzled/ lipoprotein receptor-related protein (LRP) heterodimeric receptor complexes, whereas the intact destruction complex associates with phosphorylated LRP. After this, the destruction complex captures and phosphorylates  $\beta$ -catenin, however ubiquitination is blocked. Thus,  $\beta$ -catenin stabilizes, accumulates and translocates to the nucleus. Next,  $\beta$ -catenin associates with T-cell factor/lymphoid enhancer-binding factors (TCF/LEF) transcription factors for target gene transcription, such as *AXIN2* and leucine-rich repeat-containing G-protein coupled receptor 5 (*LGR5*).

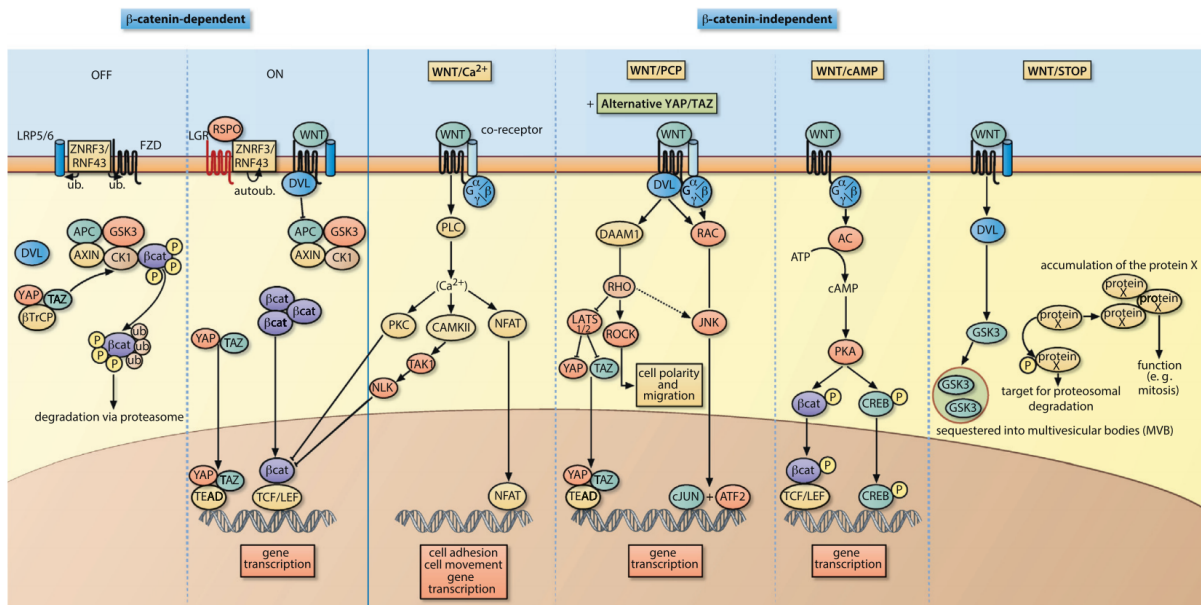


**Figure 1.5.** Schematic summary of the Wnt signaling pathway (Skronska-Wasek, Gosens, Konigshoff & Baarsma, 2018).

### 1.2.1. Wnt signaling in lung development, injury and repair

The human lung has three main developmental phases. The first, embryonic phase, goes from around weeks 4 to 7 of the embryonic stage, the second, fetal phase, goes from weeks 5 to 17 of embryonic stage and the third, the postnatal, goes from birth (~38 weeks of embryonic stage) to 3 years of age (Schittny, 2017). The lung grows approximately until the ages of 10 and 12 years and further matures until the age of 20 for females and 25 for males (Brandsma, de Vries, Costa, Woldhuis, Konigshoff & Timens, 2017). Lung development starts centrally at the conducting airways and progresses into the periphery by the formation and enlargement of the gas exchange area, and microvascular maturation. Very specific differential expression of factors from different signaling pathways, such as Wnt, fibroblast growth factors (FGF), bone morphogenic protein (BMP), and transforming growth factor beta (TGF- $\beta$ ), provide instructions for branching morphogenesis. Wnt signaling is critical for lung development, where absence has

shown to lead to lung agenesis (Goss et al., 2009; Harris-Johnson, Domyan, Vezina & Sun, 2009; Yin et al., 2008). After lung maturation, lung function progressively declines with age as a consequence of lung changes both in structure and physiology, as presented in the beginning of this section. The alveolar compartment of the lung is indispensable for life, so there is great interest in understanding its cellular composition and how to regenerate the thin interface for gas exchange after injury. Different studies suggest the lung remains largely quiescent after development, but that upon injury, multiple cell types are able to proliferate and restore the lung structure (Butler, Loring, Patz, Tsuda, Yablonskiy & Mentzer, 2012; Liu et al., 2019; Nabhan, Brownfield, Harbury, Krasnow & Desai, 2018; Zacharias et al., 2018). A wide-range of cell lineages can be stimulated to proliferate, de- or re-differentiate, and even modify their phenotype to repair an injured lung area. (Zepp & Morrissey, 2019). Wnt proteins are crucial during these processes as they are responsible for regulating stem cell maintenance and cell self-renewal (Figure 1.6.).

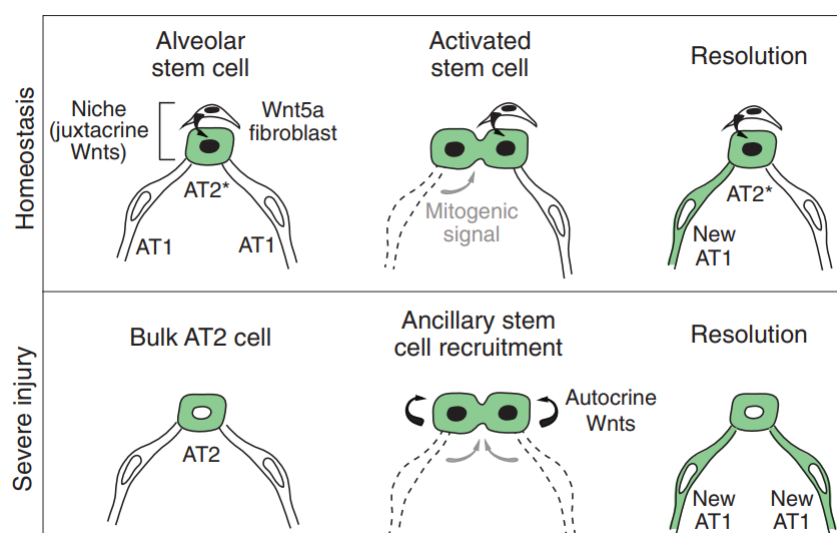


**Figure 1.6.** Schematic model of alveolar cell niche during homeostasis and injury (Nabhan, Brownfield, Harbury, Krasnow & Desai, 2018). Alveolar type 1 (AT1) and type 2 (AT2) cells.



---

### 1.2.2. Wnt signaling in COPD

In COPD, an exhausted and defective alveolar epithelial repair has been associated with recurring toxic exposure and Wnt signaling dysregulation (Basil et al., 2020). We and others have shown it to be decreased in COPD (Baarsma et al., 2017; Jiang et al., 2016; Kneidinger et al., 2011; Skronska-Wasek et al., 2017; Uhl et al., 2015; Wang et al., 2011). The decrease in Wnt signaling has been associated with alveolar type II cells, adult lung alveolar stem cells, which display inactive Wnt/  $\beta$ -catenin signaling in COPD (Figure 1.7.).

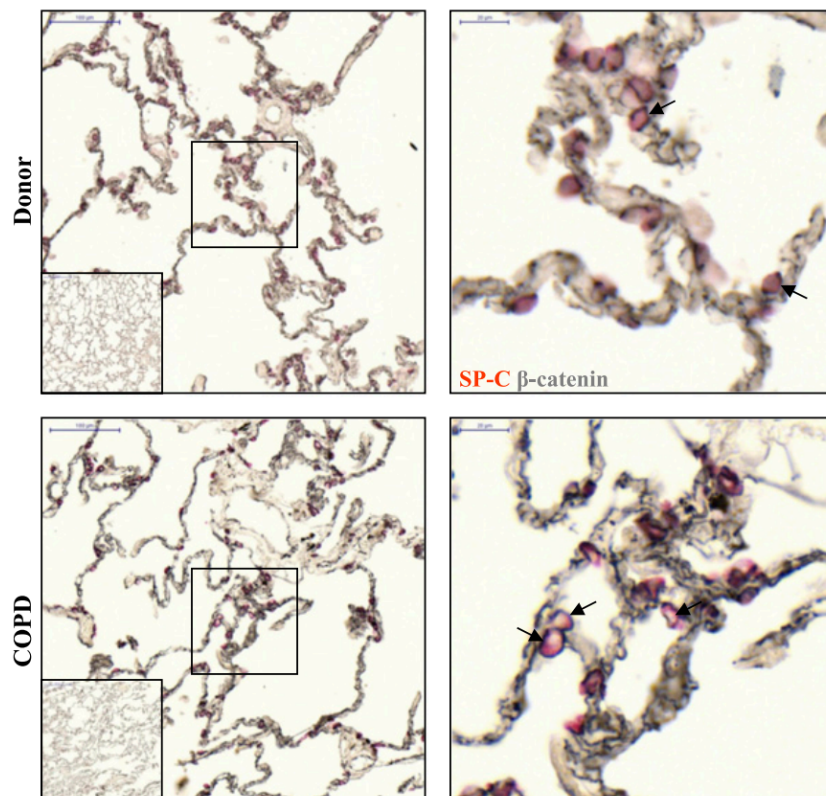


**Figure 1.7.** Immunohistochemistry staining of type II alveolar epithelial cells, demarked by SPC in red, and  $\beta$ -catenin, in grey, of lung sections obtained from non-diseased patients, donor, and COPD patients (Kneidinger et al., 2011).

We have also previously demonstrated that Wnt/ $\beta$ -catenin signaling is a promising target for lung repair in COPD/emphysema both in *in vivo* and *ex vivo* studies,

using precision-cut lung slices derived from COPD patients (Figure 1.8.) (Kneidinger et al., 2011; Uhl et al., 2015).

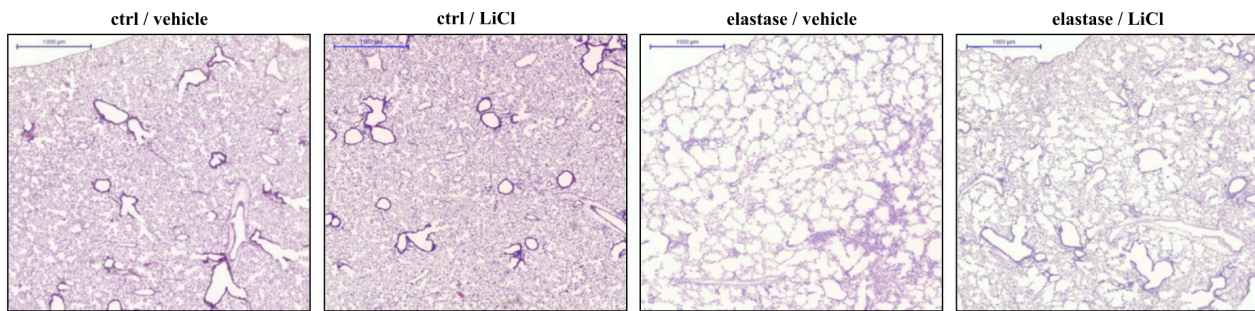


**Figure 1.8.** Hematoxylin and eosin staining of mice lung sections showing that lithium chloride (LiCl) *in vivo* administration attenuates emphysema changes in mice challenged with elastase (Kneidinger et al., 2011).

Wnt activation has been previously achieved experimentally using lithium chloride (LiCl) and CHIR99021, two well-known GSK-3 $\beta$  inhibitors. However, there are toxicity concerns in regards to their systemic use in humans (De Meyer et al., 2011; Uhl et al., 2015).

### 1.2.3. Wnt signaling modulation

As briefly mentioned above, it is possible to pharmacologically target the Wnt signaling pathway (Figure 1.9.). The interaction between different Wnt signaling components can be interrupted, resulting in either inhibition or activation of the pathway. For instance, the interaction of transcription factors TCF/LEF with  $\beta$ -catenin can be disrupted by various compounds including, PKF115-584 and iCRT14, and lead to pathway inhibition (Gonsalves et al., 2011; Yeganeh et al., 2013).

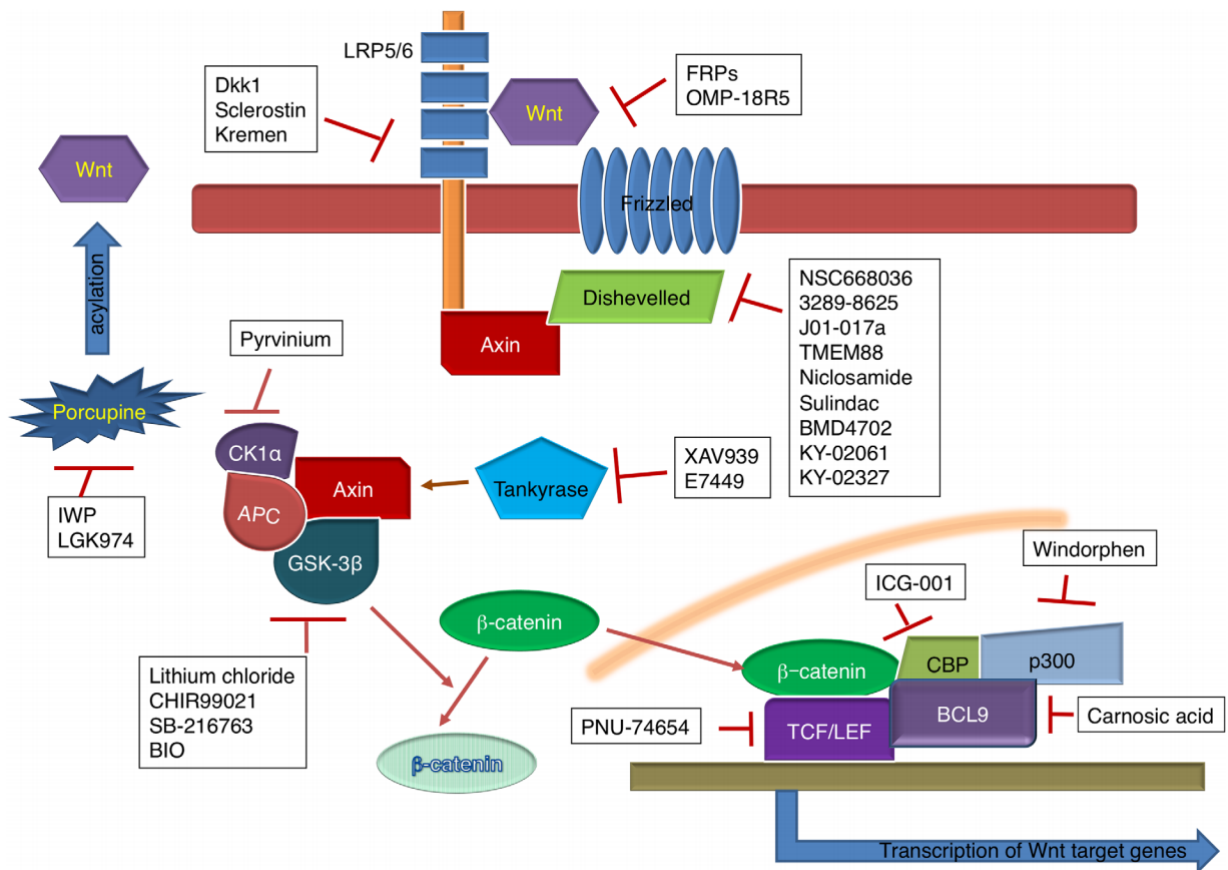


**Figure 1.9.** Small molecule inhibitors of different Wnt/β signalling pathway components (Tran & Zheng, 2017).

There is a broad interest in modulating Wnt signaling therapeutically, not only for COPD, but also for diseases like cancer, osteoporosis, Parkinson's disease and lung fibrosis (Baarsma & Konigshoff, 2017; Zimmerman, Moon & Chien, 2012). However, Wnt remains challenging as a target due to its complexity both in terms of multiple players and in terms of crosstalk with other signaling pathways, such as Hedgehog, Notch and TGF-β (Borggreffe, Lauth, Zwijsen, Huylebroeck, Oswald & Giaimo, 2016). In addition, modulation of Wnt through activation or inhibition of different protein pathways can prompt unique responses in different cell types (Anastas & Moon, 2013). Like during organ development, a strongly regulated and spatio-temporal control of gene expression is necessary for the development of therapies targeting Wnt signaling.



---

## 2. Hypothesis and aims

There is evidence that the lung has a regeneration potential after development. In COPD, endogenous repair capacity of the human diseased lung is diminished, however there are studies indicating that the remaining lung tissue is capable of responding to novel treatment options, such as Wnt/ $\beta$ -catenin activation.

The hypothesis of this PhD thesis is that Wnt/ $\beta$ -catenin exogenous activation can regenerate emphysematous lung tissue and that this can be achieved by repurposing FDA-approved compounds which can activate the Wnt pathway. Thus, the main aim of this study was to identify a safe and effective compound for Wnt/ $\beta$ -catenin signaling activation in the lung which is able to induce lung repair in the context of lung emphysema.

We defined the following subaims:

- 1) to develop a robust and reliable cell-based high-throughput compound screen, using a luciferase Wnt reporter cell line;
- 2) to identify drug candidates able to activate Wnt/ $\beta$ -catenin signaling;
- 3) to select drugs based on their protein target prediction and confirmatory assays;
- 4) to validate them in a relevant preclinical model of lung tissue regeneration;
- 5) to test the efficacy of a final candidate *in vivo*.



---

### 3. Materials and methods

#### 3.1. Cell culture

Leading Light Wnt Reporter cells (Enzo Life Sciences) and NIH/3T3 (ATCC CRL-1658, ATCC) cells were cultured in high glucose Dulbecco's Modified Eagle Medium, DMEM (Gibco), supplemented with 4 mM L-alanyl-L-glutamine dipeptide (Gibco), 10% (v/v) fetal bovine serum, FBS (PAN-Biotech) and 100 U/ml penicillin and streptomycin (Gibco). For all experiments using NIH/3T3 and Leading Light Wnt Reporter cells, well plates were coated with poly-L-lysine (Sigma-Aldrich). Briefly, culture surfaces were aseptically covered with poly-L-lysine for 5 min., solution was aspirated and plates were thoroughly rinsed with 1x sterile phosphate buffered saline solution, PBS pH 7.4 (Thermo Fisher Scientific). Wells were allowed to dry at least for 2 h before introducing cells and medium. MLg (ATCC CCL206, ATCC) cells were cultured in DMEM/Ham's F12 media (Gibco) supplemented with 10% (v/v) FBS, 100 U/ml penicillin and streptomycin. All cells were expanded in T-75 cm<sup>2</sup> flasks (Thermo Fisher Scientific) made from polystyrene (PS) and grown at 37°C with 5% CO<sub>2</sub> in humidified conditions, using a CO<sub>2</sub> cell Incubator BBD6620 (Thermo Fisher Scientific). For cell detachment, cells were rinsed with 1x PBS and incubated with 1 ml of 0.25 % Trypsin-EDTA for 5 minutes at 37°C. Trypsin activity was neutralized with 10 ml of 10% FBS growth media. Cell suspension was transferred to a 50 ml conical tube (BD Bioscience) and centrifuged for 5 minutes at 300 g and room temperature, using a centrifuge Rotina 420R (Hettich). Next, supernatant was carefully aspirated. For cryopreservation, 1 x 10<sup>6</sup> cells were suspended in freezing medium composed by 10% (v/v) dimethyl sulfoxide, DMSO (Carl Roth), 40% (v/v) media and 50% (v/v) FBS, and kept in a Liquid nitrogen cell tank BioSafe 420SC (Cryotherm). Cell

numbers were calculated using a Neubauer chamber, trypan blue 0.4% solution (Sigma-Aldrich) at a 1:2 dilution and the following formula: cell concentration (number of cells/ml of cell suspension) = (number of cells counted x 10.000) / number of squares counted. For all liquid pipetted volumes, either sterile measuring pipettes (Greiner bio-one) of single use (5 ml, 10 ml, 25 ml, 50 ml) were used with the help of PIPETGIRL (Integra) or filter tips (Biozym Scientific) were used (10 $\mu$ l, 100 $\mu$ l, 200 $\mu$ l and 1000 $\mu$ l) with fixed volume, single channel Research Plus pipettors (Eppendorf). To achieve sterile conditions, tissue culture was performed under a laminar flow hood Herasafe KS (Thermo Fisher Scientific).

### 3.2. Reagents

CHIR99021 (Tocris), amlexanox (Cayman Chemical), nabumetone, phenazopyridine hydrochloride, tolnaftate (Santa Cruz Biotechnology) and tiaprofenic acid (Sigma-Aldrich) were all dissolved in DMSO to a stock concentration of 20mM. PKF115-584 and iCRT14 (Tocris) were dissolved in DMSO to a stock concentration of 1 mM and 75 mM respectively. Lithium chloride (Sigma-Aldrich) was dissolved in culture media to a stock solution of 2 M. Reagents were stored as stock solution at -20 °C, using a freezer MediLine LGex 410 (Liebherr).

### 3.3. High-throughput small compound screen

For the compound screen, Leading Light Wnt Reporter Cell Line stably expressing firefly luciferase under the control of T-cell factor/lymphoid enhancer-binding factors (TCF/LEF) was used. 1 x 10<sup>4</sup> cells in 50 $\mu$ l of 10% (v/v) FBS supplemented



---

media were dispensed in tissue culture treated and sterilized white opaque 384-well plates (PerkinElmer) and allowed to adhere for 24 hours at 37°C in 5% CO<sub>2</sub> in humidified conditions. Cells were serum starved with 0.1% (v/v) FBS media for 24 hours to allow for cell synchronization prior to treatment. Cells were afterwards treated for 24 hours with 1,216 10 µM of compounds belonging to the Prestwick Chemical Library (Prestwick chemical) in 0.1% (v/v) FBS-supplemented medium, without replicates. 1% (v/v) DMSO, and 10 µM CHIR99021 were used as negative and positive controls, respectively, each dispensed in the first and last well plate columns (replicates of 16 wells). Media was removed and 25 µl of Bright-Glo Luciferase Assay System (Promega) was added to each well. Luminescence was measured using an EnVision 2102 Multilabel Reader (PerkinElmer). The quality and robustness of the assay was calculated using the Z' factor and the signal window (Zhang, Chung & Oldenburg, 1999). Hit threshold was set above plate average signal of the compounds plus 3 times the standard deviation. The compound library treatment was distributed in four different experiments. For this, same passage number of cells was used to guaranty consistency between cell batches.

### **3.4. Drug selection**

Computational exclusion of potential false positives was performed by chemical structure comparison of compounds active in both the high-throughput small compound screen and in multiple assays, publically available in PubChem and ChemBank databases. c (Liu & Campillos, 2014). The activity of compounds in the PubChem bioassays was taken as provided by the database. After drug exclusion,

based on compound promiscuity, drug targets were predicted with high confidence (>50% precision), using the software HitPick (Liu, Vogt, Haque & Campillos, 2013). Final candidate drugs were selected based on the number 1) of hits of a Pubmed literature search composed by: “predicted target” + “COPD” or “predicted target” + “Wnt”; and 2) of predicted targets belonging to the gene ontology terms “epithelial cell proliferation” (GO:0050673) and “regulation of inflammatory response” (GO:0050727), relevant in COPD.

### **3.5. Luciferase reporter assay**

6 x 10<sup>4</sup> Leading Light Wnt Reporter cells were seeded in each well of a 48 well plate (TPP Techno Plastic Products), flat bottom made from polystyrene (PS), 0.875 cm<sup>2</sup> growth area, 10.6 mm diameter, suspended in 250µl of 10% (v/v) FBS supplemented phenol red free media. Cells were allowed to adhere for 24 hours at 37°C in 5% CO<sub>2</sub> in humidified conditions. Next, cells were serum starved with 0.1% (v/v) FBS media for 24 hours to allow for cell synchronization prior to treatment. Cells were afterwards treated for 24 hours with 0.5, 1, 5 and 10 µM of either amlexanox, phenazopyridine hydrochloride, tolnaftate, nabumetone and tiaprofenic acid alone or in combination with 1 µM PKF115-584, a Wnt inhibitor. 0.05% (v/v) DMSO was used as negative control, and 1 µM CHIR99021 and 10mM LiCl, two Wnt inducers, were used as positive controls. Plates were stored at -80 °C turned upside down, in a freezer U570 HEF (New Brunswick) until further processing. Cells were then lysed with 65 µl of Glo Lysis Buffer (Promega) for 30 minutes at room temperature in an orbital shaker Duomax 1030 (Heidolph). After scraping and thorough mixing, 25 µl of lysate was transferred to a 96 white opaque

---

microplate (Corning), flat bottom, untreated and made from PS. Luciferase activity was determined using the software Tristar MicroWin 2000, version 4.41 (Berthold Technologies), a luminescence microplate reader (Berthold Technologies) with an automatic injection and shaking system, which dispensed 100  $\mu$ l of Bright-Glo Luciferase Assay System to the lysates and shook plates before each value acquisition. The measured values were analyzed with WinGlow Software (Berthold Technologies) and normalized to control. Quantifications were based on at least 3 independent experiments, each condition performed in triplicates.

### **3.6. Cell viability assay**

Cell viability analysis was performed using CellTiter-Glo (Promega) according to the manufacturer's instructions, in NIH/3T3 cells.  $2.5 \times 10^4$  cells were seeded in each well of a 96 well plate (TPP Techno Plastic Products), flat bottom, made from PS, with a 0.322 cm<sup>2</sup> growth area, 6.40 mm in 100  $\mu$ l 10% (v/v) FBS growth media. The assay was performed after 24h of compound treatment and measurements were done in triplicates using a luminescence plate reader. The measured values were analyzed with WinGlow Software and normalized to control. Quantifications were based on at least 3 independent experiments, each condition performed in triplicates.

### **3.7. Animals**

Eight to twelve weeks old pathogen-free wild type mice weighing 20 to 22 g were used in this study. C57BL/6N mice were purchased from Charles River Laboratories (Sulzfeld, Germany) and C57BL/6J mice from The Jackson

Laboratory (Maine, USA). Animals were housed in rooms maintained at constant temperature and humidity, with a 12 hour light cycle, and were allowed food and water *ad libitum*. Experiments were conducted under strict governmental and international guidelines, according to the regulatory guidelines of University of Colorado Institutional Animal Care and Use Committee. Animal studies are reported in compliance with the ARRIVE guidelines (Kilkenny, Browne, Cuthill, Emerson, Altman & Group, 2010).

### **3.8. Mouse lung epithelial cell isolation**

Lung epithelial cells were isolated as previously described (Messier, Mason & Kosmider, 2012; Mutze, Vierkotten, Milosevic, Eickelberg & Konigshoff, 2015; Ng-Blichfeldt et al., 2018) with slight modifications. C57BL/6N female mice were anaesthetized with a mixture of 300 mg/kg body weight ketamine (Bela-pharm) and 100 mg/kg body weight xylazine (cp-pharma), sacrificed, through exsanguination by cutting the vena cava, and lungs were flushed with PBS. Mouse lungs were intratracheally inflated with dispase (BD Bioscience) followed by 300 µl instillation of 1% (w/v) low gelling temperature agarose (A9414, Sigma Aldrich). Lungs were harvested, minced and filtered through 100 µm, 20 µm and 10 µm nylon meshes (Sefar) with the help of surgical scissors and forceps (Fine Science Tools). White blood cells were depleted with CD45 and epithelial cells were selected using CD326 (EpCAM) magnetic beads respectively (130–052-301, 130–105-958, Miltenyi Biotec), according to manufacturer's instructions, using manual separators for magnetic cell isolation (Miltenyi Biotec). EpCAM<sup>+</sup> cells were resuspended in DMEM containing 2 mM L-alanyl-L-glutamine dipeptide (Gibco), 100 U/ml penicillin and streptomycin, and (Sigma Aldrich), 3,6 mg/ml glucose (Applichem) and 10 mM

---

HEPES (Thermo Fisher Scientific) and left on ice until further use. Primary mouse lung epithelial cells were either used in the organoid assay or seeded in 6 well plates (TPP Techno Plastic Products).

### **3.9. Murine lung organoid culture**

Organoids were cultured as previously described (Barkauskas et al., 2013; Ng-Blichfeldt et al., 2018) with some modifications. Briefly, MLg mouse lung fibroblasts were proliferation-inactivated by incubation in culture medium containing 10µg/ml mitomycin C (Merck) for 2 h, followed by 3 washes in warm PBS, and let to recover in culture media for at least 1 hour. 20,000 primary lung epithelial cells (EpCAM<sup>+</sup> cells) suspended in 50 µl growth factor-reduced Matrigel (Corning) were diluted 1:1 with 20,000 MLg cells in 50µl DMEM/F12 containing 10% (v/v) FBS and seeded into 24-well plate tissue culture treated transwells inserts (Corning) with 0.4 µm pore size, made from polyester (PET) membrane, growth area 0.3 cm<sup>2</sup> and 6.4 mm diameter. Cultures were maintained in DMEM/F12 containing 5% (v/v) FBS, 100 U/ml penicillin and streptomycin, 2 mM L-alanyl-L-glutamine dipeptide (Gibco), 2.5 µg/ml amphotericin B (Gibco), 1x insulin-transferrin-selenium (Gibco), 0.025 µg/ml recombinant human epidermal growth factor, EGF (Sigma), 0.1 µg/ml cholera toxin (Sigma-Aldrich), 30 µg/ml bovine pituitary extract (Sigma-Aldrich) and 0.01 µM of freshly added all-trans retinoic acid (Sigma-Aldrich) beneath the inserts. 10 µM Y-27632 (Tocris) was added to the media for the first 48 hours of culture. Treatments were added to the organoid media from day 0 and in every culture media exchange. Media was refreshed every 2-3 days.

### 3.10. Organoid quantification

Microscopy for organoid quantification at day 14 was performed using a microscope Axiovert 40 (Zeiss). Individual organoids from multi-layer Z-stacks, with a minimum size of 50  $\mu\text{m}$ , were manually selected using the Fiji image processing package (Schindelin et al., 2012). The total number of organoids was then normalized to treatment control.

### 3.11. Immunofluorescence

Immunofluorescence staining of organoids was done as previously described (Ng-Blichfeldt et al., 2018). Organoids were kept in well inserts and fixed at day 14 with ice-cold acetone-methanol mixed 1:1 (AppliChem) for 15 minutes at  $-20^{\circ}\text{C}$ . Next, organoids were blocked with 5% (w/v) BSA (Sigma-Aldrich) dissolved in PBS, and further stored at  $4^{\circ}\text{C}$ . The following day, organoids were incubated with primary antibodies diluted in PBS with 0.1% (w/v) BSA and 0.1% (v/v) Triton X-100 solution (AppliChem) at  $4^{\circ}\text{C}$ . The next day, organoids were washed with PBS and incubated with secondary antibodies, diluted 1:200 at  $4^{\circ}\text{C}$ . Finally, on the third day cell nuclei were stained with 4'-6-diamidino-2-phenylindole, DAPI, (Roche) diluted 1:1000 for 10 minutes. Antibodies and dilutions used were: E-Cadherin 1:200 (610181, BD Bioscience), prosurfactant protein C 1:100 (AB3786, Millipore), acetylated alpha tubulin 1:2000 (ab24610, Abcam), donkey anti-mouse IgG conjugated with Alexa Fluor 647 1:200 (ab150107, Abcam), goat anti-mouse IgG conjugated with Alexa Fluor 568 1:200 (A11031, Invitrogen) and goat anti-rabbit IgG conjugated with Alexa Fluor 488 1:200 (ab150077, Abcam). Immunofluorescence was visualized using either a confocal microscope LSM710

---

or a microscope Axio Imager M2 (Zeiss). Images were processed using ImageJ (Schindelin, Rueden, Hiner & Eliceiri, 2015).

### **3.12. Amlexanox preparation and *in vivo* administration**

Amlexanox was administered to C57BL/6J mice by oral gavage as previously described (Reilly et al., 2013). Amlexanox was first dissolved in 150 mM NaOH, to a final concentration of 20 mg/ml. The solution was further diluted using a 1:1 mixture of water and 1.5 M tris(hydroxymethyl)-aminomethane hydrochloride, Tris-HCl buffer pH 8.8, to achieve a final concentration of 10 mg/mL, which was further buffered to a pH of > 7.5 solution, to avoid amlexanox precipitation. Same solution without amlexanox was used as vehicle control. Mice were treated on a daily basis, from Day -1 (the day before of elastase instillation) to Day 6, in a preventive regimen, with either 25 or 50 mg/kg amlexanox. Mice were randomized and divided into the following groups: diseased controls (elastase), diseased treated mice (elastase plus amlexanox treatment). Experiments were performed twice, once with 25 mg/kg of amlexanox and once with 50 mg/kg, with 10 animals per group (5 male and 5 female). 2 of the mice died before the end of the experiment, due to the lung injury, resulting in a final n of 9 for each of the amlexanox treatments groups.

### **3.13. Elastase mouse model of emphysema**

Emphysema was induced as described previously (Kneidinger et al., 2011). Elastase is an enzyme known to induce destruction of lung tissue. The elastase-

induced injury model is widely used to study emphysema and well documented (Wright, Cosio & Churg, 2008). Shortly, porcine pancreatic elastase (Sigma-Aldrich) was dissolved in sterile PBS (Gibco) and applied orotracheally (4U/100g body weight in 80  $\mu$ l PBS) in 3% isoflurane anaesthetized C57BL/6J mice. Animal health status and weights were closely monitored on a daily basis.

### **3.14. Lung function measurement**

C57BL/6J mice were anaesthetized with ketamine-xylazine, tracheostomized, intubated and connected to a FlexiVent FX system (SCIREQ) (John-Schuster et al., 2014). Mice were ventilated with a tidal volume of 10 ml/kg at a frequency of 150 breaths/minute to reach a mean lung volume similar to that of spontaneous breathing. Testing of lung mechanical properties including dynamic lung compliance and resistance was carried out by a software-generated script. Measurements were repeated four times per animal. The coefficient of determination (COD), a quality control parameter comparing the experimental signals and the lung function software models, was determined by the system. Only datasets with a coefficient higher than 0.95 were included in the analysis. Following lung function measurements, anaesthetized animals were sacrificed and lungs were harvested.

### **3.15. Blinding**

To decrease unintentional bias, personnel was blinded to experimental groups during sample processing and data analysis of animal experiments. During the



---

blinding process, samples were randomly excluded so that sample sizes were the same between treatment groups during processing and analysis.

### **3.16. RNA extraction, cDNA synthesis and quantitative real-time PCR**

Total RNA from cells was isolated using the peqGOLD Total RNA Kit (Peqlab), according to the manufacturer's instructions. Fresh lung tissue was snap frozen in liquid nitrogen, with the help of a nitrogen container (KGW Isotherm) and kept at  $-80\text{ }^{\circ}\text{C}$  until further processing. Frozen tissue was pulverized using a TissueLyser II (Qiagen), 7 mm steel beads (Qiagen) in 2 ml safe-lock reaction tubes (Eppendorf) at a frequency of  $25\text{ s}^{-1}$  for 1 minute. Total RNA from lung tissue homogenate was isolated using QIAzol (Qiagen) and purified with the peqGOLD Total RNA Kit (Peqlab), using a centrifuge Mikro 200 (Hettich). RNA was quantified using a NanoDrop 1000 (PeqLab).  $1\text{ }\mu\text{g}$  of RNA in  $20\text{ }\mu\text{l}$  RNase/DNase free water (Gibco) was denatured at  $72\text{ }^{\circ}\text{C}$  for 10 minutes in a Mastercycler nexus (Eppendorf). cDNA was synthesized by reverse transcription, using  $2.5\text{ U}/\mu\text{l}$  M-MLV Reverse Transcriptase (Invitrogen), 1X First Strand Buffer (Invitrogen),  $10\text{ mM}$  DTT (Invitrogen),  $2.5\mu\text{M}$  random hexamers (Invitrogen),  $0.5\text{ mM}$  of nucleotide (dNTP) mix (Thermo Scientific), and  $1\text{ Unit}/\mu\text{l}$  RNase inhibitor (Thermo Scientific). Incubation at  $20\text{ }^{\circ}\text{C}$  for 10 min. was followed by an annealing cycle at  $43\text{ }^{\circ}\text{C}$  for 75 min and an extension at  $99\text{ }^{\circ}\text{C}$  for 5 min and left at  $4^{\circ}\text{C}$  for cooling down, in a PCR reaction. cDNA was diluted 1:5 with water and stored at  $-20\text{ }^{\circ}\text{C}$ . mRNA expression of target genes was compared with reference control hypoxanthine-guanine phosphoribosyltransferase (Hprt)-1, using SYBR Green (Roche) and a LC480 Light Cycler (Roche). Primers were used at a final concentration of  $500\text{ nM}$  with

the following sequences: *Hprt* forward 5'-CCTAAGATGAGCGCAAGTTGAA-3', reverse 5'-CCACAGGACTAGAACACCTGCTAA-3', *Axin2* forward 5'-AGCAGAGGGACAGGAACCA-3', reverse 5'-CTGAACCGATTCATGACCAC-3', *Lgr5* forward 5'-GCGTTCACGGGCCTTCACAG-3', reverse 5'-GGCATCTAGGCGCAGGGATTGA-3', *Fgf7* forward 5'-AGGCTCAAGTTGCACGAGGC-3', reverse 5'-GCGGTTGCTCCTTGACTTTTGT-3', *Hgf* forward 5'-TGCCTGTGCCTTGACTTAGCG-3', reverse 5'-CCGGGCTGAAAGAATCAAAGCA-3', *Adamts4* forward 5'-AACCAAGCGCTTCGCTTCTCT-3', reverse 5'-AGCTGCCATAACCGTCAGCA-3', *Eln* forward 5'-GGCGTCTTGCTGATCCTCT-3', reverse 5'-ATAATAGACTCCACCGGGA-3', *Mmp12* forward 5'-TGTACCCACCTACAGATACCTTA-3', reverse 5'-CCATAGAGGGACTGAATGTTACGT-3'. The reaction conditions used for the qPCR were: initial denaturation for 5 min. at 95 °C, followed by 45 cycles of denaturation for 5 s. at 95 °C, annealing for 5 s. at 59 °C and elongation for 10s. at 72 °C, followed by a cycle step for melting curve analysis to acquire the dissociation characteristics of double-stranded DNA, for 5 s. at 95 °C, 1 min. at 60 °C and a continuous acquisition from 60-95 °C, ending and a final cooling step at 4 °C. Relative transcript expression of a gene was calculated as difference between cycle threshold, ct ( $\Delta Ct = Ct \text{ reference gene} - Ct \text{ target gene}$ ).

---

### **3.17. Statistical analysis**

Data were analyzed with GraphPad Prism 8.0. and presented as mean  $\pm$  SD. n refers to number of independent experiments. The statistical tests used are stated in the figure legends in the results section.

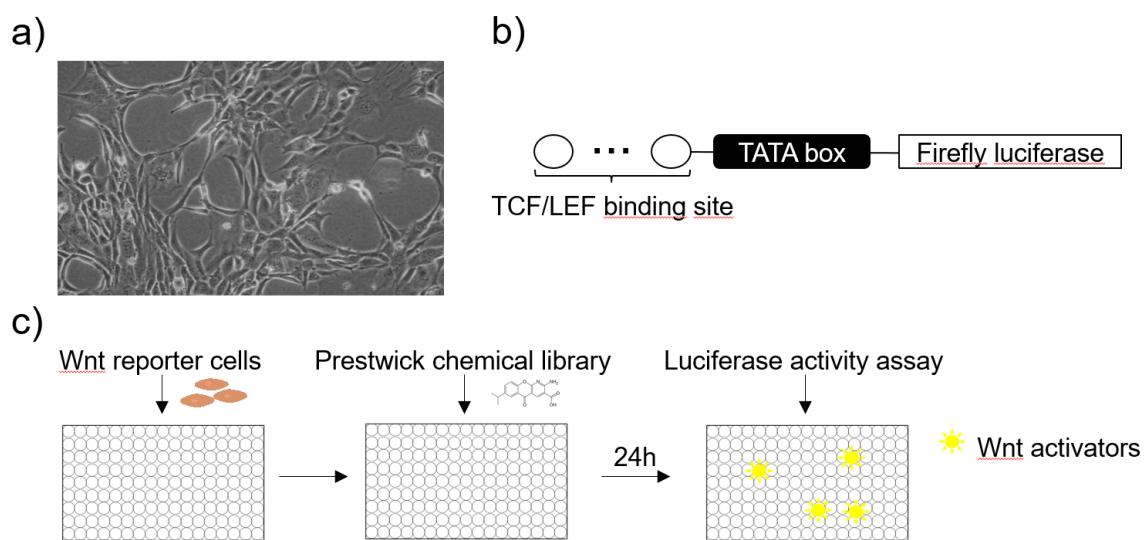


---

## 4. Results

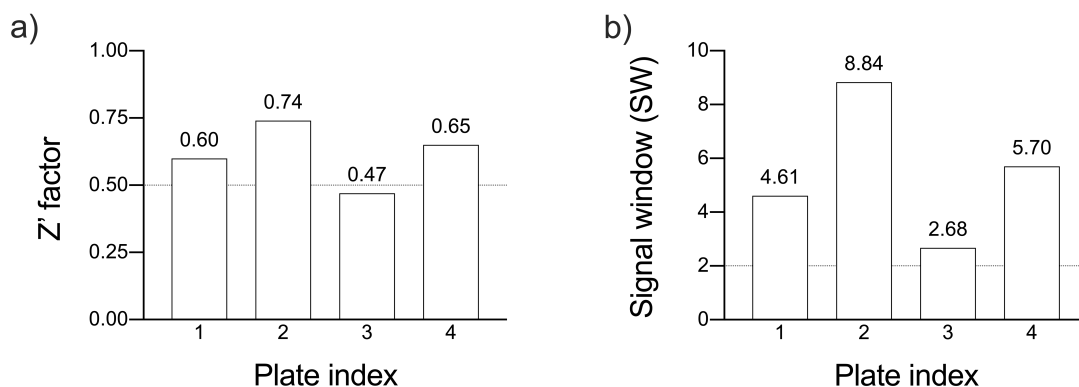
### 4.1. Wnt/ $\beta$ -catenin luciferase reporter cell based screening identifies human approved drugs as Wnt activators

To discover a pharmaceutical which could activate Wnt/ $\beta$ -catenin signaling, we screened 1216 clinical approved drugs by the European Medicine Agency (EMA), Food and Drug Administration (FDA) and other agencies, using a Wnt luciferase reporter cell line (Figure 4.1.).



**Figure 4.1.** Cell-based Wnt/ $\beta$ -catenin reporter high-throughput drug screening. **a)** Phase-contrast image of Leading Light Wnt Reporter Cell Line used for the drug screen. **b)** Schematic of DNA construct stably expressed in the Leading Light Wnt Reporter Cell Line. The firefly luciferase reporter gene is under the control of a basal promoter element, TATA box, joined to tandem repeats of a proprietary and non-disclosed Wnt-responsive elements (TCF/LEF binding site). **c)** Experimental design of the drug screening. Leading Light Wnt Reporter Cell Line was seeded in 384 well-plates, serum starved (0.1% FBS containing media) for 24 hours, and treated for another 24 hours with 10  $\mu$ M of each compound, using the Prestwick chemical library, consisting of 1216 approved drugs. Luciferase assay was performed, luminescence values were analyzed and luciferase activity was calculated relative to control (1% DMSO). 10 $\mu$ M CHIR99021 was used as positive control.

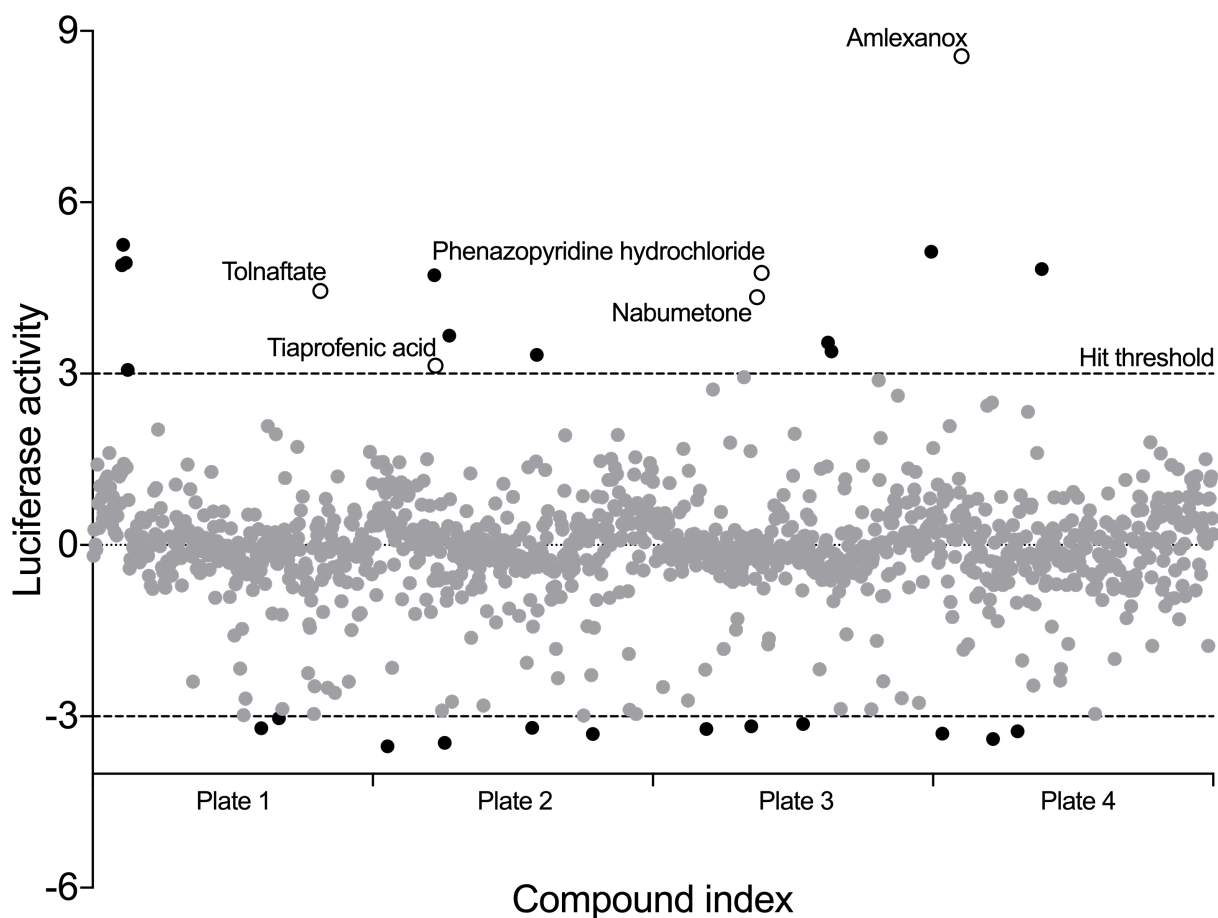
The quality metrics for our high-throughput screen were determined by the Z' factor and the signal window, which were calculated for the four different plates, run on different days (Figure 4.2.). The Z'-factor is a parameter that takes into account the signal means and standard deviations, being highly sensitive to data variability. The assay is accepted if this value is greater than 0.4 (Zhang, Chung & Oldenburg, 1999). The signal window is used to estimate the uniformity and separation of the upper and lower signals of the assay. When this parameter is greater than 2, the assay is considered acceptable. As an outcome of our validation process, we accepted the results of all four plates, as both robust and reliable.



**Figure 4.2.** High-throughput assay quality metrics, calculated for each assay plate. **a)** Z' factor and **b)** signal window.

We identified 16 drugs that increased  $\beta$ -catenin-dependent luciferase activity (Figure 4.3.). 12 drugs were in the Wnt inhibitory range of the assay, but were not further explored, as this was not within the aims of this project.

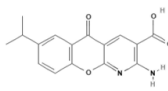
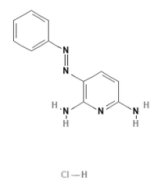
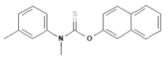
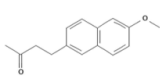
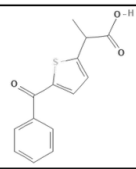
The hit threshold for our assay was set above the mean signal of the general compound signal, shifted by three times the standard deviation, specific for each assay plate.



**Figure 4.3.** Luciferase assay results of the Wnt/ $\beta$ -catenin reporter high-throughput drug screening. Compound screen identified 16 Wnt/ $\beta$ -catenin/TCF/LEF activators. Hits Z-score was set as greater than the average signal of all compounds plus three times the standard deviation. White dots highlight the five selected candidate compounds: amlexanox, phenazopyridine hydrochloride, tolnaftate, nabumetone and tiaprofenic acid.

For further analysis, we selected five candidate compounds from the 16 hits (Table 4.1.). The selected compounds amlexanox, phenazopyridine hydrochloride, tolnaftate, nabumetone and tiaprofenic acid had different Wnt induction capacities in our drug screen. Furthermore, the candidate drugs have different chemical structures and belong to different therapeutic classes, except for phenazopyridine, nabumetone and tiaprofenic acid, which all target the central nervous system.

**Table 4.1.** Candidate compound summary.

Drug	Therapeutic class	Formula	Structure	Luciferase activity
Amlexanox	Allergology	$C_{16}H_{14}N_2O_4$		8.6
Phenazopyridine hydrochloride	Central Nervous System	$C_{11}H_{12}ClN_5$		4.8
Tolnaftate	Infectiology	$C_{19}H_{17}NOS$		4.5
Nabumetone	Central Nervous System	$C_{15}H_{16}O_2$		4.3
Tiaprofenic acid	Central Nervous System	$C_{14}H_{12}O_3S$		3.1

The selection of the five drugs was based on a promiscuity analysis in ChemBank and PubChem databases and in the hit predicted protein targets (Figure 4.4.). From the 16 hits, 12 and 15 were previously tested in other assays and results are publicly available in the ChemBank and PubChem databases, respectively. Regarding the predicted protein targets of our hits, from the total 16 candidates, it was possible to identify predicted targets for 15 hits. These 15 hits to which it was possible to identify predicted protein targets, differed from the 15 hits with described bioassay activity in the PubChem database.



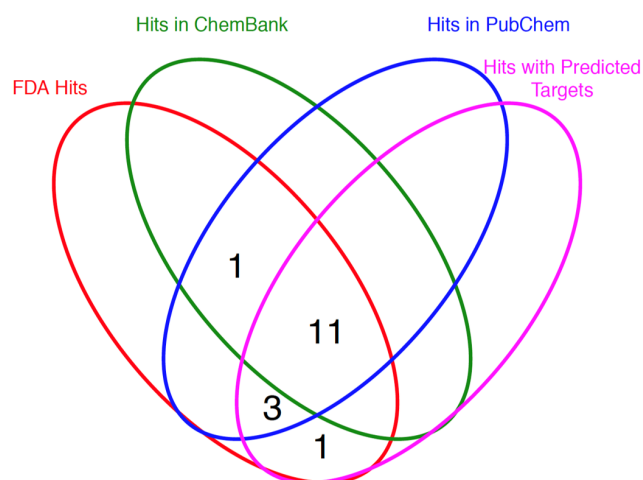


**Figure 4.4.** Venn diagram showing the overlap of hits to compounds tested in ChemBank and PubChem bioassay databases, as well as compounds with predicted targets.

In detail, the promiscuity analysis took into account the activity information available in public screen repositories. For this, we calculated the ratio between the number of assays in which the hits were tested and the number of assays in which the hits were active (Table 4.2.) in comparison with our 16 hits. Tiaprofenic acid lacked bioassay activity information reported in the public sets. For amlexanox, no data regarding bioassay activity could be retrieved from the ChemBank database.

**Table 4.2.** Summary of promiscuity analysis of final five selected candidate drugs.

Drugs	Promiscuity in bioassays (%)	
	PubChem	ChemBank
<b>Amlexanox</b>	6,9 (active in 35 of 501 screens)	-
<b>Phenazopyridine hydrochloride</b>	7,5 (active in 86 of 1189 screens)	4,1 (active in 29 of 697 screens)
<b>Tolnaftate</b>	2,7 (active in 33 of 1219 screens)	2,7 (active in 18 of 654 screens)
<b>Nabumetone</b>	2,8 (active in 33 of 1154 screens)	1,7 (active in 11 of 647 screens)
<b>Tiaprofenic acid</b>	-	-

For the prediction of each candidate protein target, we used the bioinformatic tool HitPick (Figure 4.5.). HitPick combines two methods for target prediction. One based on the compounds' 2D molecular fingerprint which calculates a Tanimoto coefficient, accounting for the most similar compound from a database. The second, a Bayesian model, generates a ranked list of target predictions of known ligand–target interactions of the most similar compound.

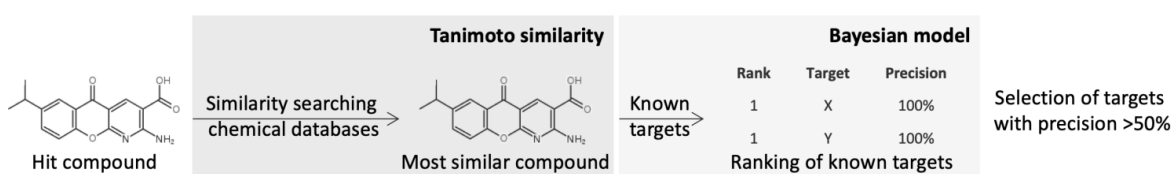


**Figure 4.5.** Schematic of HitPick protein target prediction strategy (Liu et al., 2013).

40 With the predicted protein targets, we performed a literature Pubmed search using the keywords “Wnt” or “COPD” or the GO terms “epithelial cell proliferation” or “regulation of inflammatory response” (Table 4.3.). Amlexanox’s targets were the most associated with all four criteria. Predicted targets for phenazopyridine hydrochloride and tolnaftate were associated with “COPD” and “regulation of inflammatory responses”. Nabumetone and tiaprofenic acid targets were both associated with “Wnt” or “COPD” and “regulation of inflammatory response”. According to this selection strategy, although all five compounds induced Wnt/β-catenin signaling, the targets of only three compounds were associated with “Wnt”.

**Table 4.3.** Summary of literature search of the final five selected candidates drugs.

Drugs	Keywords		Gene ontology terms	
	Wnt	COPD	Epithelial cell proliferation	Regulation of inflammatory response
Amlexanox	+	+	+	+
Phenazopyridine hydrochloride	-	+	-	+
Tolnaftate	-	+	-	+
Nabumetone	+	+	-	+
Tiaprofenic acid	+	+	-	+

#### **4.2. Inhibition of $\beta$ -catenin reduces Wnt dependent luciferase activity in amlexanox and phenazopyridine hydrochloride treated cells**

Next, we aimed at confirming the candidate drugs amlexanox, phenazopyridine hydrochloride, tolinaftate, nabumetone and tiaprofenic acid, selected in our primary screen. First, we wanted to validate that the identified drugs regulated specifically  $\beta$ -catenin signaling. To do so, we treated the Wnt reporter cells with four different concentrations of the candidate drugs alone or together with PKF115-584, a well-known compound, inhibiting the T cell factor (TCF)- $\beta$ -catenin complex (Lepourcelet et al., 2004). In all single compound treatments, there was a significant increase in luciferase activity, confirming the results of our drug screen. Wnt induction was achieved in all compound concentrations, except for the lower dose of tiaprofenic acid. Inhibition of  $\beta$ -catenin led to a significant decrease in luciferase activity only in amlexanox and phenazopyridine treatments (Figure 4.6.). For tolinaftate, nabumetone and tiaprofenic acid, there was also a decrease in luciferase activity, but not significant. At the same time, we observed that lithium chloride (LiCl), a classic inhibitor of GSK-3 $\beta$  and only patient-experienced drug known to activate Wnt/ $\beta$ -catenin signaling, could induce luciferase activity in our

reporter system, but had a lower luciferase activity induction compared to the candidate drugs.

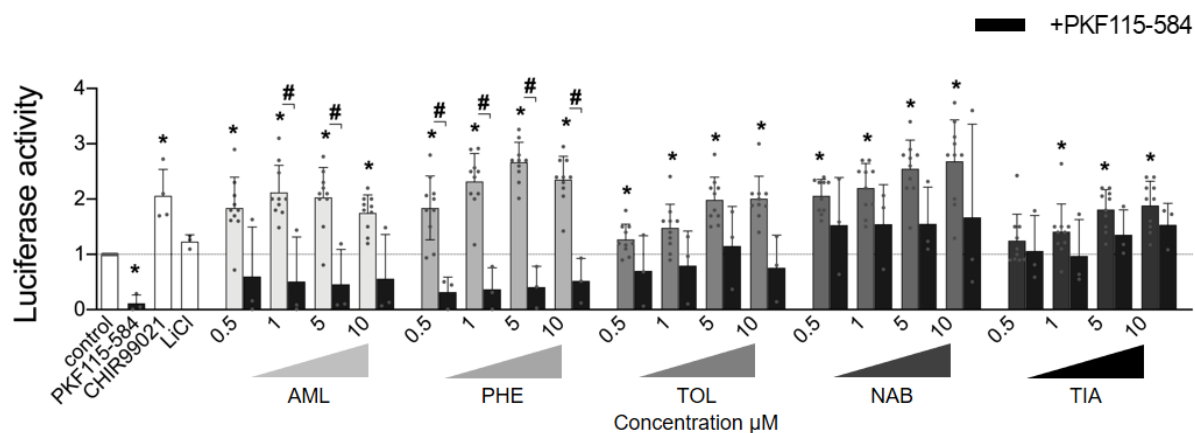


**Figure 4.6.** Luciferase assay in Leading Light Wnt Reporter Cell Line treated with 0.5, 1, 5, or 10  $\mu\text{M}$  of candidate compounds for 24 hours with or without 1  $\mu\text{M}$  PKF115-584, calphostin C, an antagonist of TCF/ $\beta$ -catenin complex. GSK-3 $\beta$  inhibitors, 1  $\mu\text{M}$  CHIR99021 and 10mM LiCl were used as positive controls. Luciferase activity was calculated relative to negative control (DMSO).  $n=3-10$ . One sample t-test to a hypothetical value of 1,  $*p<0.05$ , and One-way ANOVA,  $\#p<0.05$ . Data is presented as mean  $\pm$  SD of independent experiments. Control (DMSO), lithium chloride (LiCl), amlexanox (AML), phenazopyridine hydrochloride (PHE), tolinaftate (TOL), nabumetone (NAB) and tiaprofenic acid (TIA).

Second, the five selected candidate hits were analyzed in a dose dependent manner with respect to their proliferative capacity, to rule out the possibility that the increase in luciferase activity was due to an increase in cell number (Figure 4.7.). We observed that there were no significant changes in the metabolic activity of the cells treated with the candidate drugs, measured by ATP levels, accounting both for proliferation and toxicity. Cell proliferation was only observed in the CHIR99021 treated cells. Based on these results, we continued our investigation with the compounds amlexanox and phenazopyridine hydrochloride.

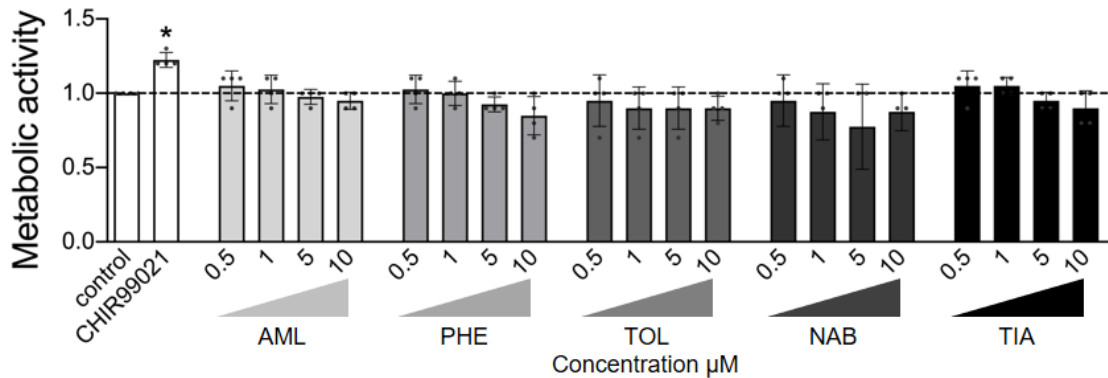


**Figure 4.7.** Metabolic activity of NIH/3T3 cells treated with 0.5, 1, 5, or 10  $\mu\text{M}$  of candidate compounds for 24 hours was evaluated by ATP levels, measured with cell titer glo luminescent cell viability assay. 1  $\mu\text{M}$  CHIR99021 was used as a positive control. Metabolic activity was calculated relative to negative control (DMSO).  $n=4$ . One sample t-test to a hypothetical value of 1,  $*p<0.05$ . Data is presented as mean  $\pm$  SD of independent experiments. Control (DMSO), lithium chloride (LiCl), amlexanox (AML), phenazopyridine hydrochloride (PHE), tolinaftate (TOL), nabumetone (NAB) and tiaprofenic acid (TIA).

### 4.3. Amlexanox and phenazopyridine hydrochloride induce primary adult epithelial cell derived organoid formation

We next investigated the implications of the candidate drugs amlexanox and phenazopyridine hydrochloride, which showed previous specificity for  $\beta$ -catenin activation, in lung regeneration, using adult mouse epithelial cells in a 3D organoid assay (Figure 4.8.). We tested the increased capability of epithelial progenitor cells co-cultured with MLg lung fibroblasts cell line in matrigel to form organoids by two different concentrations of each compound, 0.5 and 1  $\mu\text{M}$ , which proved to be sufficient to induce Wnt signaling in the Wnt reporter luciferase assay.

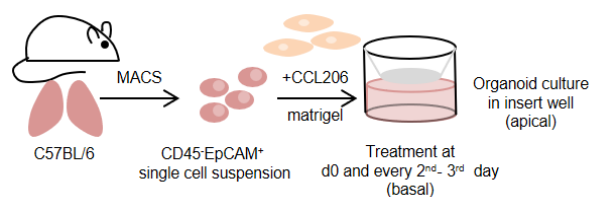


**Figure 4.8.** Schematic of mouse organoid experimental setup. Primary mouse ATII cells were isolated from 10-12 weeks old wild type C57BL/6 mice lungs after

enzymatic dissociation with dispase and MACS sorting of CD45 negative and EpCAM positive cells. Cells were seeded in matrigel together with non-proliferative MLg lung fibroblasts in well inserts. Media with treatments was changed every second to third day. Organoid cultures were maintained for 14 days. Adapted from Lehmann et al. (Lehmann et al., 2020).

We observed significant differences in organoid formation between each treatment (Figure 4.9.).

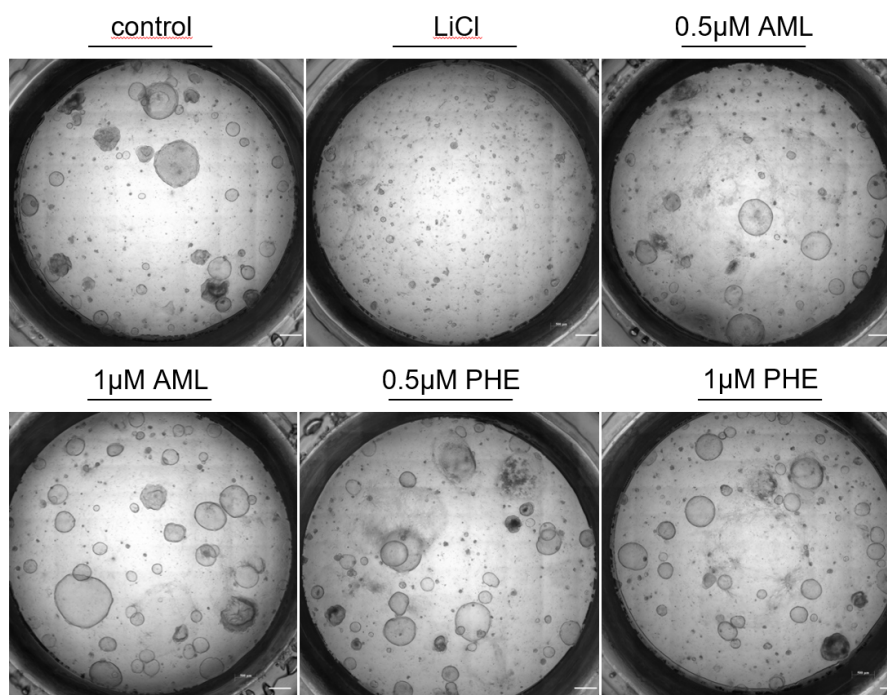


**Figure 4.9.** Representative phase contrast images of whole insert organoids (top) and inset images (bottom). Treatments with DMSO, 10 mM LiCl, 0.5 and 1 µM amlexanox and 0.5 and 1 µM phenazopyridine hydrochloride started at day 0 and continued every 2nd to 3rd day for 14 days. Scale bar=500µm.

Organoid formation capacity was induced by LiCl, amlexanox and lower doses of phenazopyridine hydrochloride (Figure 4.10.).

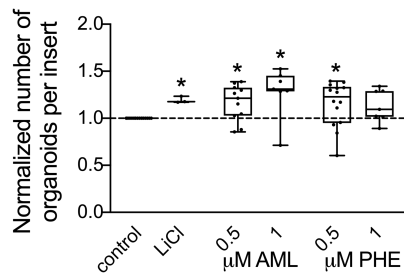


**Figure 4.10.** Normalized total number of organoids per insert to control (DMSO). n=3-14. One sample t-test to a hypothetical value of 1, \*p<0.05. Data is presented as mean ± SD of independent experiments. Lithium chloride (LiCl), amlexanox (AML) and phenazopyridine hydrochloride (PHE).

Interestingly, we saw in parallel that primary adult epithelial cells cultured in 2D conditions were more responsive to compound Wnt activation than the MLg lung fibroblasts used in the organoid assay (Figures 4.11. and 4.12.). This Wnt augmented responsiveness was observed by a non-significant increase in Wnt target genes, *Axin2* and *Lgr5* (Figure 4.11.).

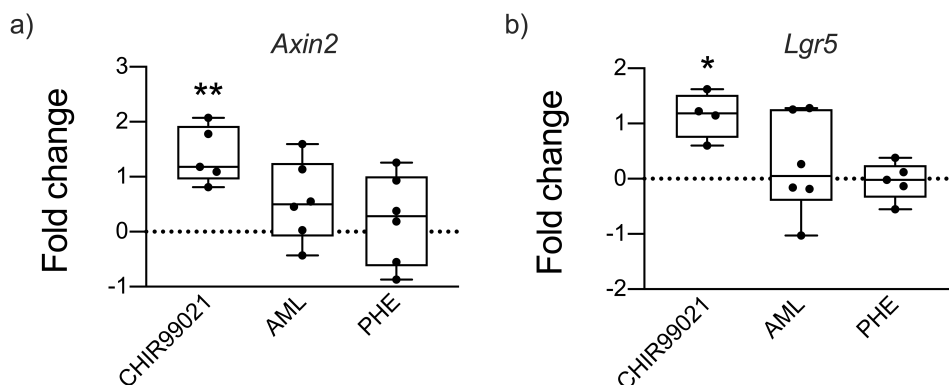


**Figure 4.11.** Wnt target gene expression analysis in mouse adult lung epithelial cells cultured 2D. **a)** *Axin2* and **b)** *Lgr5*. Cells were treated for 24 hours with either 2 μM of CHIR99021, 0.5 μM of amlexanox (AML) or 0.5 μM of phenazopyridine hydrochloride (PHE). n=4-6. Data is presented as mean ± SD of independent experiments. One sample t-test to a hypothetical value of 0, \*p<0.05.

Wnt induction in MLg mouse lung fibroblasts was only consistently achieved with CHIR99021 (Figure 4.12.).

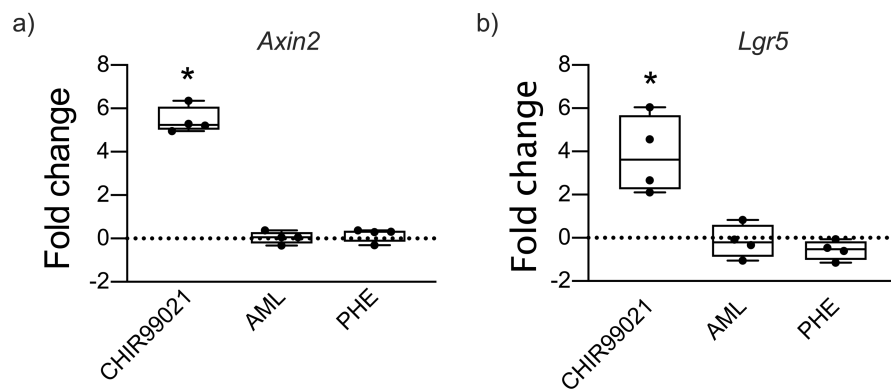


**Figure 4.12.** Wnt target gene expression analysis in MLg mouse lung fibroblast cell line. **a)** *Axin2* and **b)** *Lgr5*. Cells were treated for 24h with either 2  $\mu\text{M}$  of CHIR99021, 0.5  $\mu\text{M}$  of amlexanox (AML) or 0.5  $\mu\text{M}$  of phenazopyridine hydrochloride (PHE).  $n=4$ . Data is presented as mean  $\pm$  SD of independent experiments. One sample t-test to a hypothetical value of 0,  $*p<0.05$ .

Furthermore, in the organoid cultures, we observed that compound treatment for 14 days did not alter E-cadherin expression, indicating no disruption of cell to cell adhesion which is observed in some cancers where Wnt is dysregulated (Figure 4.13.).

46

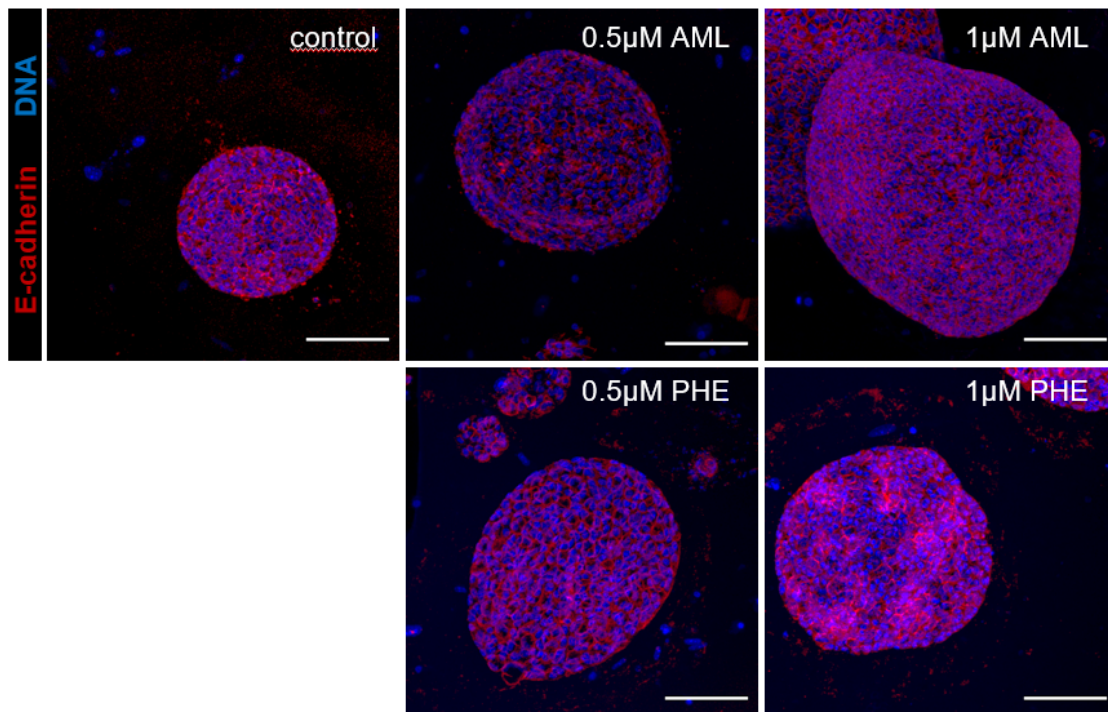


**Figure 4.13.** Maximum intensity projection images of whole mount immunofluorescence stainings of day 14 organoids. E-cadherin (red) and DAPI (blue). Scale bar=100 $\mu\text{m}$ .



Organoids expressed lung epithelial cell markers acetylated alpha tubulin (ACT) and pro-surfactant C protein (SFTPC), markers for airway and alveolar epithelial cells respectively, as highlighted by the red and green arrows (Figure 4.14.). These results show the contribution and importance of progenitor cells to airway as well as alveolar lung repair.

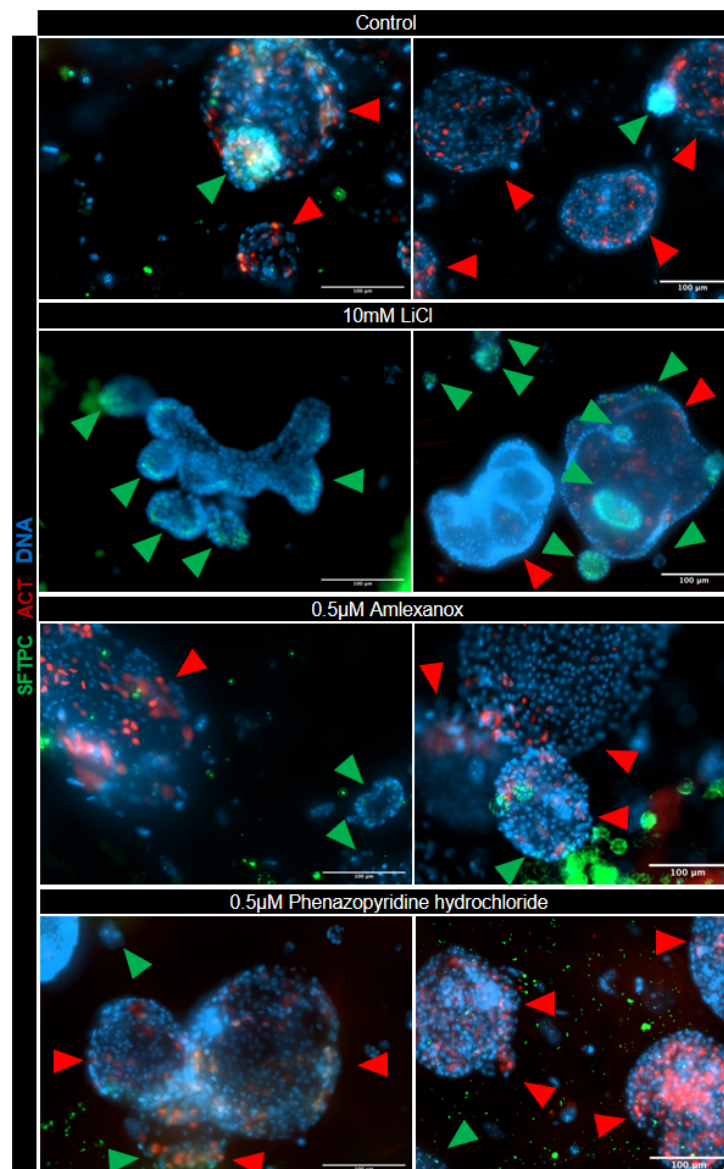


**Figure 4.14.** Images from whole mount immunofluorescent stained day 14 organoids. Pro-surfactant protein C (SFTPC, green), acetylated alpha tubulin (ACT, red) and DAPI (DNA, blue). Scale bar=100µm. Lithium chloride (LiCl), amlexanox (AML) and phenazopyridine hydrochloride (PHE).

#### 4.4. Inhibition of $\beta$ -catenin reduces amlexanox and phenazopyridine hydrochloride organoid formation capacity

Lung epithelial cell progenitor capability to form organoids *in vitro* requires Wnt/ $\beta$ -catenin signaling (Hu et al., 2020). We next determined whether the Wnt pathway is functionally required for amlexanox and phenazopyridine hydrochloride to induce organoid formation. For this we used another known potent Wnt inhibitor iCRT14, which interferes with TCF binding to DNA in addition to influence TCF/ $\beta$ -catenin interaction (Gonsalves et al., 2011) (Figure 4.15.).

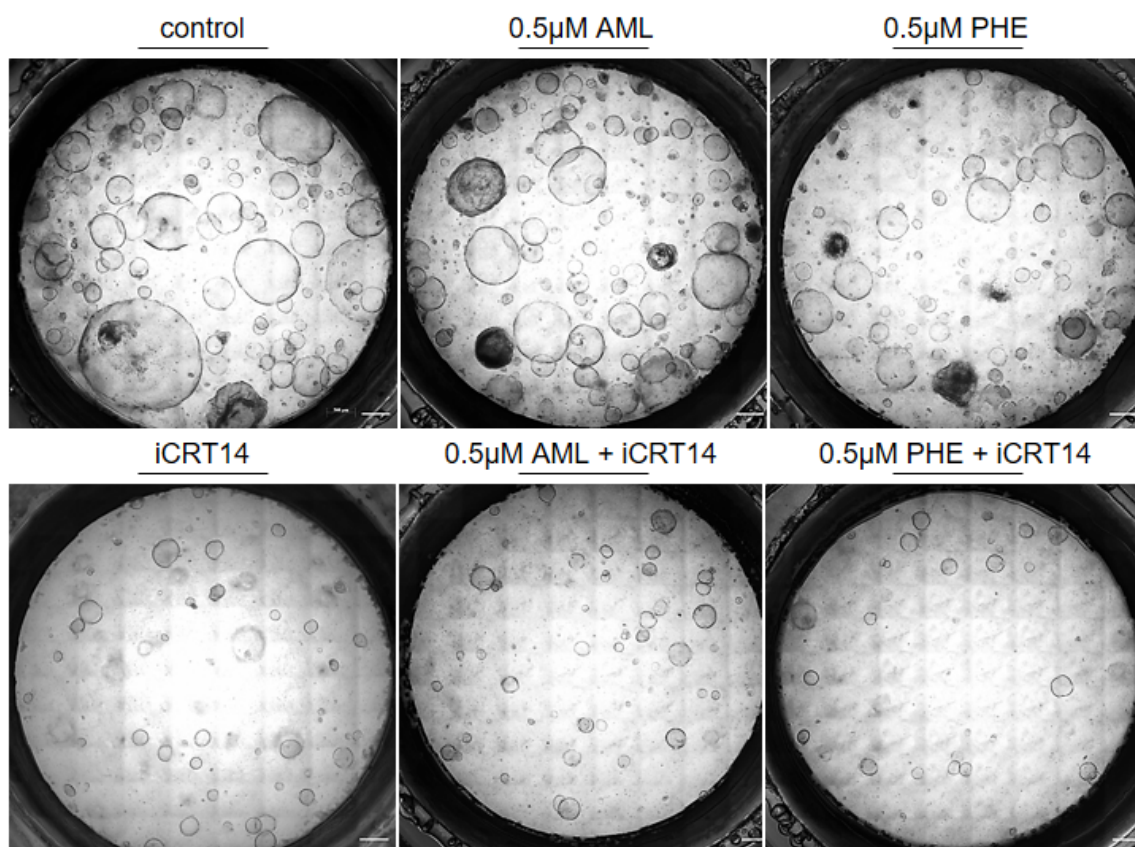


**Figure 4.15.** Representative phase contrast images of whole insert day 14 organoids after 0.5  $\mu$ M candidate compound treatment amlexanox and phenazopyridine hydrochloride with or without 10  $\mu$ M iCRT14, a potent Wnt inhibitor which blocks  $\beta$ -catenin/TCF4 binding. Scale bar=500 $\mu$ m.

---

iCRT14 organoid treatment, significantly reduced organoid numbers when used alone or in combination with amlexanox or phenazopyridine hydrochloride (Figure 4.16.). These data further support the notion that the positive effect of the compounds on organoid formation is due to Wnt signaling.

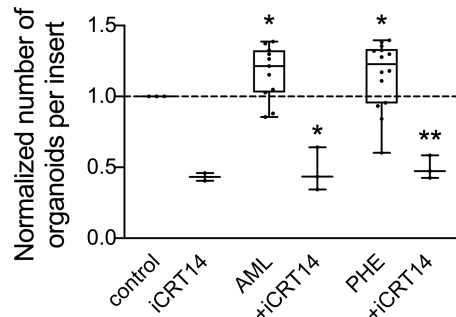


**Figure 4.16.** Normalized total number of organoids per insert to control (DMSO). n=2-14. Data is presented as box plots with median of independent experiments. One sample t-test to a hypothetical value of 1, \*p<0.05, \*\*p<0.01. Amlexanox (AML) and phenazopyridine hydrochloride (PHE).

#### 4.5. Amlexanox treatment improves lung function and induces Wnt related genes while reducing disease markers in a mouse model of lung emphysema

Since amlexanox performed better in the organoid assay than phenazopyridine hydrochloride, we selected amlexanox for further investigation. We next investigated whether the regenerative effect observed with amlexanox in primary adult lung epithelial cell derived organoid cultures could also be observed *in vivo* (Figure 4.17.). We started a daily treatment of amlexanox and induced COPD like changes in mouse lungs with elastase orotracheal administration. Animals were treated preventively, as performed previously (Kneidinger et al., 2011), with vehicle, 25 or 50 mg/kg of amlexanox twice before being challenged with elastase, and additionally for 7 days post injury.

## Results

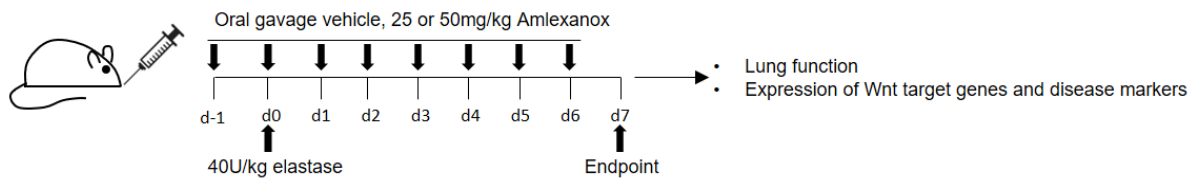


**Figure 4.17.** Schematic overview of wild type C57BL/6 mice treated with amlexanox. Mice were treated preventively either with 25, 50mg/kg of amlexanox or vehicle a day before being challenged with 40U/kg of body weight of porcine pancreatic elastase and every day for 7 days via oral gavage. Lung function and gene expression was analyzed.

Animals treated preventively with 50 mg/kg of amlexanox a day before being challenged with elastase and for 7 days, had an improved lung function, and translated into a lower lung compliance when compared with mice treated only with vehicle or lower dose of amlexanox (Figure 4.18.).

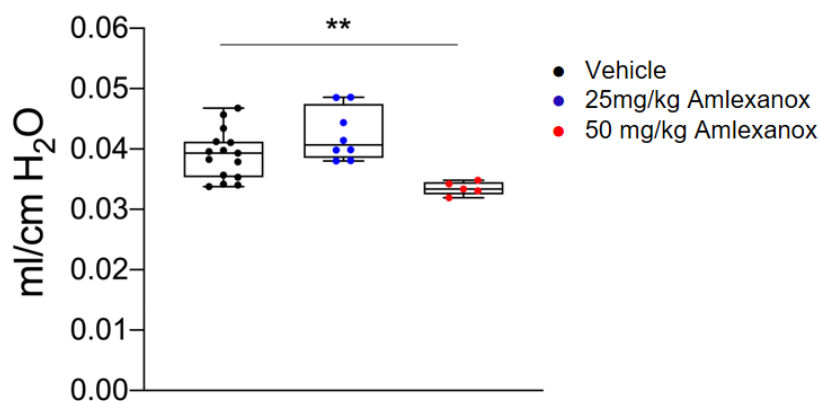


**Figure 4.18.** Dynamic compliance from lung function analysis. n=5-15. Data is presented as mean  $\pm$  SD. Mann-Whitney test, \*p<0.05, \*\*p<0.01.

Amlexanox *in vivo* treatment also induced changes in fibroblast growth factor 7 (*Fgf7*) and hepatocyte growth factor (*Hgf*) lung gene expression, which are associated with lung repair by promoting distal lung growth and branching of airways during lung development (Figure 4.19.).

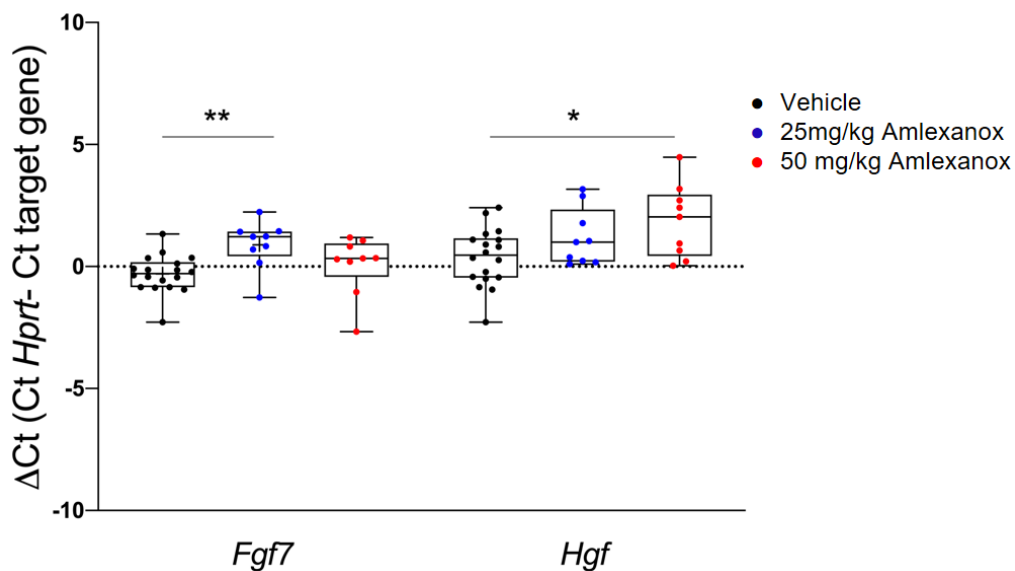


**Figure 4.19.** Lung gene expression analysis of Wnt related genes *Fgf7* and *Hgf*. n=9-18. Data is presented as mean  $\pm$  SD. Mann-Whitney test, \*p<0.05, \*\*p<0.01.

ADAM metalloproteinase with thrombospondin type 1 motif 4 (*Adamts4*) and elastin (*Eln*) lung gene expression, markers associated with COPD (Ezzie et al., 2012; Houghton et al., 2006; Uhl et al., 2015) were decreased with amlexanox treatment while *Mmp12* was increased (Figure 4.20.).

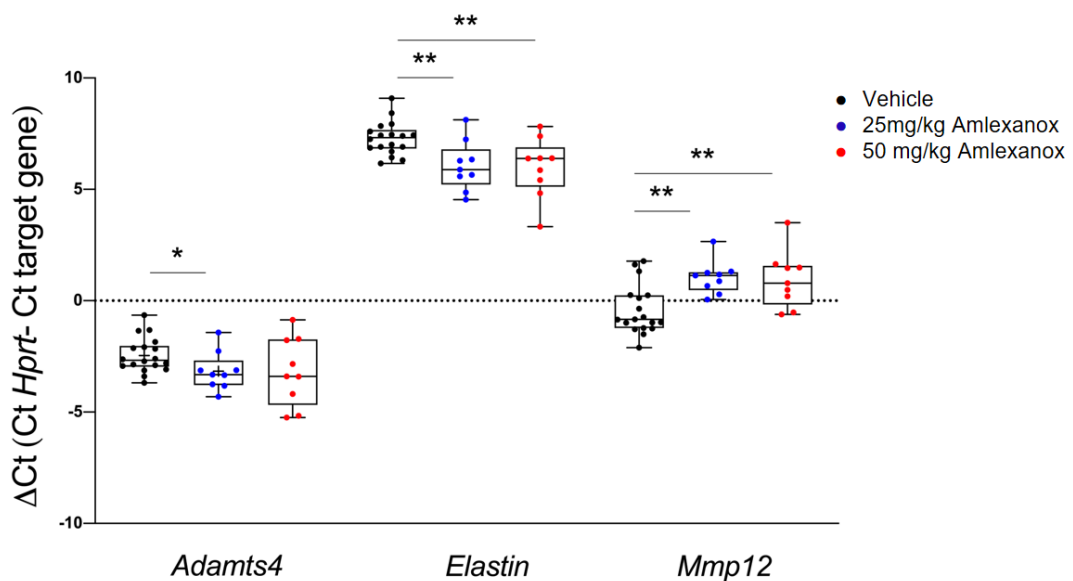


**Figure 4.20.** Lung gene expression analysis of COPD/emphysema related genes *Adamts4*, *Eln* and *Mmp12*. n=9-18. Data is presented as mean  $\pm$  SD. Mann-Whitney test, \*p<0.05, \*\*p<0.01.



---

## 5. Discussion

The field of regenerative medicine is evolving rapidly with the growing understanding of molecular and cell-specific features during organ development, injury and regeneration, provided mainly by stem cell, single cell sequencing and cell tracing studies but also by the improvement of experimental models. On the other hand, drug development is still a long process, in particular for respiratory disease, mainly due to the failure in translating compounds into human application. Currently, the importance of rapid drug discovery for finding new treatments for emerging respiratory diseases, is being highlighted every day. Drug repurposing can shorten the drug development cycle from 10-17 years to 3-12 years and represents thus an advantageous approach (Dudley, Deshpande & Butte, 2011).

Our study provides an early proof of concept for rapid drug translation. Here, we propose amlexanox for the treatment of lung emphysema and COPD. We found that amlexanox could be used for regenerative pharmacology through Wnt signaling activation.

A first unbiased drug screen, showed that 16 approved compounds induce Wnt dependent luciferase activity. Other groups, performing independent cell-based screenings, have also reported similar results, which reinforce the reproducibility of our findings (Biechele et al., 2010; Zhan et al., 2019; Zhao, Cheng, Theriault, Sheridan, Tsai & Haggarty, 2012). Only compounds which showed no promiscuity in publicly available bioassays, were further considered in our study. Next, we selected five candidate drugs based on a platform for target prediction called HitPick. Using HitPick, targets were predicted by molecular comparison of our hits to other compounds for which targets are known. After a literature search, hits in

which predicted protein targets were found to be associated with either “Wnt” or “COPD” or belonging to the GO terms “epithelial cell proliferation” or “regulation of inflammatory response” were selected. Our approach goes in line with the strategies in place for computational drug repurposing (Dudley, Deshpande & Butte, 2011). We have incorporated both drug-based strategies, through chemical similarities with other compounds for target prediction, as well as disease-based strategies, through the association of the hits’ predicted targets to current knowledge of disease and pathology, to select final drug candidates with strong potential for COPD treatment.

We focused our further analysis on amlexanox, phenazopyridine hydrochloride, tolnaftate, nabumetone and tiaprofenic acid. All five drugs, induced luciferase activity in a confirmatory screening for Wnt induction, using the same cell line we used in the initial screen. To exclude the possibility that luciferase increases were due to cell proliferation, we measured ATP changes after drug treatment. Wnt is associated with cell proliferation, but in our setup we did not observe significant increase in number of cells, as demonstrated by cell metabolic activity (Rulifson et al., 2007).

Upon Wnt inhibition, only two compounds showed a significant decrease of their Wnt induction capacity in a 2D cell culture. On the one hand, this shows Wnt specificity, but on the other hand it could represent a challenge in the disease context, where the tissue environment dampens Wnt signaling (Baarsma et al., 2017).

Our initial screen was based on results observed in embryonic fibroblasts, so we next used an organoid lung culture systems, to predict pharmacological effects



---

which could not be detected in a 2D and monoculture experimental setup. Both amlexanox and phenazopyridine hydrochloride could induce lung organoid formation, and led to differentiation of adult epithelial cell, indicating a lung regeneration potential. E-cadherin protein expression is essential in maintaining epithelial tissue and known to be reduced in many epithelial cell malignancies (Yu, Yang, Li & Zhang, 2019). In our hands, amlexanox and phenazopyridine hydrochloride did not seem to have a negative effect in e-cadherin expression in adult lung epithelial cells. We treated organoid cultures with a Wnt inhibitor and saw a significant reduction in organoid formation capacity, accounting for the rationale of this assay for studying the Wnt pathway. Since amlexanox performed better in the 3D assay than phenazopyridine hydrochloride, we moved to the next step with amlexanox.

Our *in vivo* results indicate that amlexanox treatment could initiate a pro-regenerative environment in the lung, as observed by an improvement in lung function of mice receiving high dose of amlexanox and changes in lung gene expression of *Fgf7*, *Hgf*, *Adamts4* and *Eln*. FGF7 plays an important role in human distal lung growth (Graeff, Wang & McCray, 1999), hepatocyte growth factor (HGF) has been demonstrated to be deficient in COPD (Barnes, 2014) and administration reversed emphysema in a mouse model (Hegab et al., 2008). In parallel, ADAMTS4 and elastin have been shown to be increased in emphysema (Ezzie et al., 2012; Houghton et al., 2006). We have shown previously that Wnt activation can decrease lung gene expression of MMP12, but to our surprise, *Mmp12* was increased in mice lungs after amlexanox treatment (Uhl et al., 2015). A possible explanation for this observation is the still ongoing inflammation and remodeling process, which is responsible for this increase.

Amlexanox is used for the treatment of aphthous ulcers, allergic rhinitis and asthma. The drug is anti-inflammatory and anti-allergic with immunomodulatory properties. The mechanism of action has been described to be through reduction of the release of histamine and leukotrienes (Inagaki et al., 1992). Different studies indicate that amlexanox administration is associated with weight loss and inflammation reduction. Currently, amlexanox is under clinical trial for the treatment of type 2 diabetes and obesity (NCT01842282). Amlexanox was shown to have a bronchodilator effect in aspirin-induced asthma patients. Therapeutic use of leukotrienes in COPD is known to be beneficial. Besides its regenerative potential, amlexanox could have an anti-inflammatory effect in COPD.

Only recently, a study showed that amlexanox can act as a Wnt modulator (Bordonaro & Lazarova, 2019). It is important to note that we did not explore the mechanism by which amlexanox induces Wnt signaling.

Furthermore, a recent study characterized stem cell clone libraries of COPD patient's lungs in advanced stages and identified normal lung stem cells present and three more predominant pathogenic stem cell variants (Rao et al., 2020). These stem cell variants were found to contribute to COPD, and targeting them represents an opportunity to treat the disease. This study indicates however that COPD patients retain normal lung stem cell niches that could potentially regenerate the lung. Discovery of Wnt modulators that selectively affect one or more of these cell populations could potentially induce regeneration in an adult and diseased lung.

---

## 6. Conclusion and future directions

In summary, amlexanox was selected as a candidate for the treatment of COPD based on a combination of criteria. The use of different phenotypic and computational readouts allowed us to select amlexanox as a potential lung repair drug (Figure 6.1.).

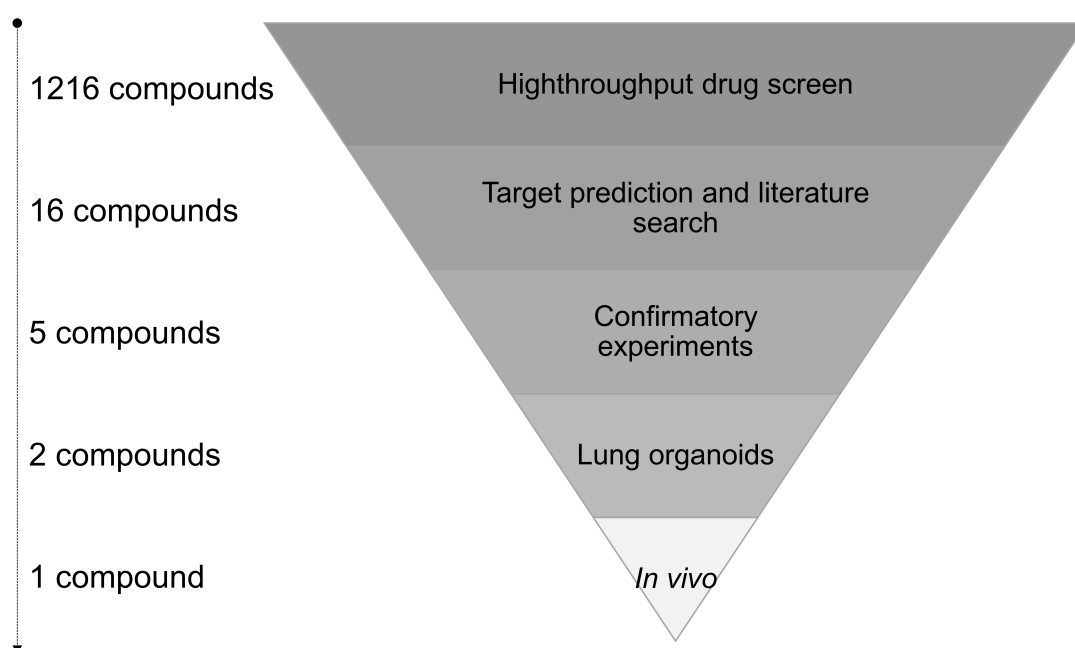


**Figure 6.1.** Summary of main strategy and outcomes of this project.

Many other undiscovered uses of drugs exist and finding these new uses is an important and necessary step towards reducing disease burden. Our study further supports the hypothesis that Wnt/ $\beta$ -catenin signaling is a target for the treatment of COPD. The use of amlexanox can lead to activation of regenerative mechanisms. Our findings advance drug discovery in the context of lung regeneration and COPD.

Although Wnt/ $\beta$ -catenin signaling hyper-activity is associated with other diseases, temporal and spatial regulation of the pathway is important in determining cellular fate (Lehmann et al., 2020). Further studies regarding regenerative potential of the adult human lung as well as the regenerative capacity of COPD patient's lungs are needed to understand the true regenerative potential of amlexanox in the lung. However, since amlexanox is an approved drug, there is the benefit of knowing already its safety, side-effects and doses for human application.

---

## 7. References

Agusti A (2014). The path to personalised medicine in COPD. *Thorax* 69: 857-864.

Agusti A (2019). COPD: Challenges and opportunities. *Respirology*.

Agusti A, & Faner R (2018). COPD beyond smoking: new paradigm, novel opportunities. *Lancet Respir Med* 6: 324-326.

Agusti A, & Faner R (2019). Lung function trajectories in health and disease. *Lancet Respir Med* 7: 358-364.

Agusti A, Faner R, Donaldson G, Heuvelin E, Breyer-Kohansal R, Melen E, *et al.* (2019). Chronic Airway Diseases Early Stratification (CADSET): a new ERS Clinical Research Collaboration. *Eur Respir J* 53.

Agusti A, & Hogg JC (2019). Update on the Pathogenesis of Chronic Obstructive Pulmonary Disease. *N Engl J Med* 381: 1248-1256.

Anastas JN, & Moon RT (2013). WNT signalling pathways as therapeutic targets in cancer. *Nat Rev Cancer* 13: 11-26.

Baarsma HA, & Konigshoff M (2017). 'WNT-er is coming': WNT signalling in chronic lung diseases. *Thorax* 72: 746-759.

Baarsma HA, Skronska-Wasek W, Mutze K, Ciolek F, Wagner DE, John-Schuster G, *et al.* (2017). Noncanonical WNT-5A signaling impairs endogenous lung repair in COPD. *J Exp Med* 214: 143-163.

Barkauskas CE, Cronce MJ, Rackley CR, Bowie EJ, Keene DR, Stripp BR, *et al.* (2013). Type 2 alveolar cells are stem cells in adult lung. *The Journal of clinical investigation* 123: 3025-3036.

Barnes PJ (2014). Hepatocyte growth factor deficiency in COPD: a mechanism of emphysema and small airway fibrosis? *Chest* 146: 1135-1136.

Basil MC, Katzen J, Engler AE, Guo M, Herriges MJ, Kathiriya JJ, *et al.* (2020). The Cellular and Physiological Basis for Lung Repair and Regeneration: Past, Present, and Future. *Cell Stem Cell* 26: 482-502.

---

Bennett JE, Stevens GA, Mathers CD, Bonita R, Rehm J, Kruk ME, *et al.* (2018). NCD Countdown 2030: worldwide trends in non-communicable disease mortality and progress towards Sustainable Development Goal target 3.4. *Lancet* 392: 1072-1088.

Bermingham ML, Walker RM, Marioni RE, Morris SW, Rawlik K, Zeng Y, *et al.* (2019). Identification of novel differentially methylated sites with potential as clinical predictors of impaired respiratory function and COPD. *EBioMedicine* 43: 576-586.

Biechele TL, Camp ND, Fass DM, Kulikauskas RM, Robin NC, White BD, *et al.* (2010). Chemical-genetic screen identifies riluzole as an enhancer of Wnt/beta-catenin signaling in melanoma. *Chem Biol* 17: 1177-1182.

Bordonaro M, & Lazarova D (2019). Amlexanox and UPF1 Modulate Wnt Signaling and Apoptosis in HCT-116 Colorectal Cancer Cells. *J Cancer* 10: 287-292.

Borggreffe T, Lauth M, Zwijsen A, Huylebroeck D, Oswald F, & Giaimo BD (2016). The Notch intracellular domain integrates signals from Wnt, Hedgehog, TGFbeta/BMP and hypoxia pathways. *Biochim Biophys Acta* 1863: 303-313.

60 Bousquet J, Dahl R, & Khaltsev N (2007). Global alliance against chronic respiratory diseases. *Allergy* 62: 216-223.

Brandsma CA, de Vries M, Costa R, Woldhuis RR, Konigshoff M, & Timens W (2017). Lung ageing and COPD: is there a role for ageing in abnormal tissue repair? *Eur Respir Rev* 26.

Butler JP, Loring SH, Patz S, Tsuda A, Yablonskiy DA, & Mentzer SJ (2012). Evidence for adult lung growth in humans. *N Engl J Med* 367: 244-247.

Cazzola M, Stolz D, Rogliani P, & Matera MG (2020). alpha1-Antitrypsin deficiency and chronic respiratory disorders. *Eur Respir Rev* 29.

Celli BR, & Wedzicha JA (2019). Update on Clinical Aspects of Chronic Obstructive Pulmonary Disease. *N Engl J Med* 381: 1257-1266.

Chitalia VC, Foy RL, Bachschmid MM, Zeng L, Panchenko MV, Zhou MI, *et al.* (2008). Jade-1 inhibits Wnt signalling by ubiquitylating beta-catenin and mediates Wnt pathway inhibition by pVHL. *Nat Cell Biol* 10: 1208-1216.

---

Clevers H, & Nusse R (2012). Wnt/beta-catenin signaling and disease. *Cell* 149: 1192-1205.

Cohen AB (1975). The interaction of alpha-1-antitrypsin with chymotrypsin, trypsin and elastase. *Biochim Biophys Acta* 391: 193-200.

Collaborators GBDCRD (2020). Prevalence and attributable health burden of chronic respiratory diseases, 1990-2017: a systematic analysis for the Global Burden of Disease Study 2017. *Lancet Respir Med* 8: 585-596.

De Meyer I, Martinet W, Van Hove CE, Schrijvers DM, Hoymans VY, Van Vaeck L, *et al.* (2011). Inhibition of inositol monophosphatase by lithium chloride induces selective macrophage apoptosis in atherosclerotic plaques. *Br J Pharmacol* 162: 1410-1423.

Decramer M, Janssens W, & Miravittles M (2012). Chronic obstructive pulmonary disease. *Lancet* 379: 1341-1351.

Dudley JT, Deshpande T, & Butte AJ (2011). Exploiting drug-disease relationships for computational drug repositioning. *Brief Bioinform* 12: 303-311.

Ezzie ME, Crawford M, Cho JH, Orellana R, Zhang S, Gelinas R, *et al.* (2012). Gene expression networks in COPD: microRNA and mRNA regulation. *Thorax* 67: 122-131.

Fagerberg L, Hallstrom BM, Oksvold P, Kampf C, Djureinovic D, Odeberg J, *et al.* (2014). Analysis of the human tissue-specific expression by genome-wide integration of transcriptomics and antibody-based proteomics. *Mol Cell Proteomics* 13: 397-406.

Fletcher C, & Peto R (1977). The natural history of chronic airflow obstruction. *Br Med J* 1: 1645-1648.

*Global strategy for the diagnosis, management, and prevention of Chronic Obstructive Pulmonary Disease 2020 Report.* [Online] Available from <https://goldcopd.org/wp-content/uploads/2019/11/GOLD-2020-REPORT-ver1.1wms.pdf>. [Accessed: 26th November 2019].

Gonsalves FC, Klein K, Carson BB, Katz S, Ekas LA, Evans S, *et al.* (2011). An RNAi-based chemical genetic screen identifies three small-molecule inhibitors of the Wnt/wingless signaling pathway. *Proc Natl Acad Sci U S A* 108: 5954-5963.

---

Goss AM, Tian Y, Tsukiyama T, Cohen ED, Zhou D, Lu MM, *et al.* (2009). Wnt2/2b and beta-catenin signaling are necessary and sufficient to specify lung progenitors in the foregut. *Dev Cell* 17: 290-298.

Graeff RW, Wang G, & McCray PB, Jr. (1999). KGF and FGF-10 stimulate liquid secretion in human fetal lung. *Pediatr Res* 46: 523-529.

Hadzic S, Wu CY, Avdeev S, Weissmann N, Schermuly RT, & Kosanovic D (2020). Lung epithelium damage in COPD - An unstoppable pathological event? *Cell Signal* 68: 109540.

Harris-Johnson KS, Domyan ET, Vezina CM, & Sun X (2009). beta-Catenin promotes respiratory progenitor identity in mouse foregut. *Proc Natl Acad Sci U S A* 106: 16287-16292.

Hegab AE, Kubo H, Yamaya M, Asada M, He M, Fujino N, *et al.* (2008). Intranasal HGF administration ameliorates the physiologic and morphologic changes in lung emphysema. *Mol Ther* 16: 1417-1426.

Heller O, Somerville C, Suggs LS, Lachat S, Piper J, Aya Pastrana N, *et al.* (2019). The process of prioritization of non-communicable diseases in the global health policy arena. *Health Policy Plan* 34: 370-383.

Higham A, Quinn AM, Cancado JED, & Singh D (2019). The pathology of small airways disease in COPD: historical aspects and future directions. *Respir Res* 20: 49.

Houghton AM, Quintero PA, Perkins DL, Kobayashi DK, Kelley DG, Marconcini LA, *et al.* (2006). Elastin fragments drive disease progression in a murine model of emphysema. *J Clin Invest* 116: 753-759.

Hu Y, Ng-Blichfeldt JP, Ota C, Ciminieri C, Ren W, Hiemstra PS, *et al.* (2020). Wnt/beta-catenin signaling is critical for regenerative potential of distal lung epithelial progenitor cells in homeostasis and emphysema. *Stem Cells*.

Inagaki M, Michimata H, Minato K, Sunaga Y, Kobayashi S, Tani G, *et al.* (1992). [Inhibitory effect of amlexanox on asthmatic attacks in an aspirin sensitive asthmatic]. *Nihon Kyobu Shikkan Gakkai Zasshi* 30: 1180-1185.

Jiang Z, Lao T, Qiu W, Polverino F, Gupta K, Guo F, *et al.* (2016). A Chronic Obstructive Pulmonary Disease Susceptibility Gene, FAM13A, Regulates Protein Stability of beta-Catenin. *Am J Respir Crit Care Med* 194: 185-197.



---

John-Schuster G, Hager K, Conlon TM, Irmeler M, Beckers J, Eickelberg O, *et al.* (2014). Cigarette smoke-induced iBALT mediates macrophage activation in a B cell-dependent manner in COPD. *Am J Physiol Lung Cell Mol Physiol* 307: L692-706.

Jonigk D, Al-Omari M, Maegel L, Muller M, Izykowski N, Hong J, *et al.* (2013). Anti-inflammatory and immunomodulatory properties of alpha1-antitrypsin without inhibition of elastase. *Proc Natl Acad Sci U S A* 110: 15007-15012.

Kerstjens HAM, Upham JW, & Yang IA (2019). Airway pharmacology: treatment options and algorithms to treat patients with chronic obstructive pulmonary disease. *J Thorac Dis* 11: S2200-S2209.

Kilkenny C, Browne W, Cuthill IC, Emerson M, Altman DG, & Group NCRGW (2010). Animal research: reporting in vivo experiments: the ARRIVE guidelines. *Br J Pharmacol* 160: 1577-1579.

Kneidinger N, Yildirim AO, Callegari J, Takenaka S, Stein MM, Dumitrascu R, *et al.* (2011). Activation of the WNT/beta-catenin pathway attenuates experimental emphysema. *Am J Respir Crit Care Med* 183: 723-733.

Kohansal R, Martinez-Cambor P, Agusti A, Buist AS, Mannino DM, & Soriano JB (2009). The natural history of chronic airflow obstruction revisited: an analysis of the Framingham offspring cohort. *Am J Respir Crit Care Med* 180: 3-10.

Lehmann M, Hu Q, Hu Y, Hafner K, Costa R, van den Berg A, *et al.* (2020). Chronic WNT/beta-catenin signaling induces cellular senescence in lung epithelial cells. *Cell Signal* 70: 109588.

Lepourcelet M, Chen YN, France DS, Wang H, Crews P, Petersen F, *et al.* (2004). Small-molecule antagonists of the oncogenic Tcf/beta-catenin protein complex. *Cancer Cell* 5: 91-102.

Liu Q, Liu K, Cui G, Huang X, Yao S, Guo W, *et al.* (2019). Lung regeneration by multipotent stem cells residing at the bronchioalveolar-duct junction. *Nat Genet* 51: 728-738.

Liu X, & Campillos M (2014). Unveiling new biological relationships using shared hits of chemical screening assay pairs. *Bioinformatics* 30: i579-586.

---

Liu X, Vogt I, Haque T, & Campillos M (2013). HitPick: a web server for hit identification and target prediction of chemical screenings. *Bioinformatics* 29: 1910-1912.

Lortet-Tieulent J, Soerjomataram I, Lopez-Campos JL, Ancochea J, Coebergh JW, & Soriano JB (2019). International trends in chronic obstructive pulmonary disease mortality, 1995-2017. *Eur Respir J*.

Martinez FJ, & Chang A (2005). Surgical therapy for chronic obstructive pulmonary disease. *Semin Respir Crit Care Med* 26: 167-191.

Meek P, Lareau S, Fahy B, & Austegard E (2019). Medicines for COPD. *Am J Respir Crit Care Med* 200: P3-P5.

Meek P, Lareau S, Fahy B, & Austergard E (2019). Surgery for Chronic Obstructive Pulmonary Disease. *Am J Respir Crit Care Med* 200: P5-P6.

Messier EM, Mason RJ, & Kosmider B (2012). Efficient and rapid isolation and purification of mouse alveolar type II epithelial cells. *Exp Lung Res* 38: 363-373.

64 Mutze K, Vierkotten S, Milosevic J, Eickelberg O, & Konigshoff M (2015). Enolase 1 (ENO1) and protein disulfide-isomerase associated 3 (PDIA3) regulate Wnt/beta-catenin-driven trans-differentiation of murine alveolar epithelial cells. *Dis Model Mech* 8: 877-890.

Nabhan AN, Brownfield DG, Harbury PB, Krasnow MA, & Desai TJ (2018). Single-cell Wnt signaling niches maintain stemness of alveolar type 2 cells. *Science* 359: 1118-1123.

Ng-Blichfeldt JP, Schrik A, Kortekaas RK, Noordhoek JA, Heijink IH, Hiemstra PS, *et al.* (2018). Retinoic acid signaling balances adult distal lung epithelial progenitor cell growth and differentiation. *EBioMedicine* 36: 461-474.

Quaderi SA, & Hurst JR (2018). The unmet global burden of COPD. *Glob Health Epidemiol Genom* 3: e4.

Randell SH (2006). Airway epithelial stem cells and the pathophysiology of chronic obstructive pulmonary disease. *Proc Am Thorac Soc* 3: 718-725.

Rao W, Wang S, Duleba M, Niroula S, Goller K, Xie J, *et al.* (2020). Regenerative Metaplastic Clones in COPD Lung Drive Inflammation and Fibrosis. *Cell* 181: 848-864 e818.

---

Reilly SM, Chiang SH, Decker SJ, Chang L, Uhm M, Larsen MJ, *et al.* (2013). An inhibitor of the protein kinases TBK1 and IKK- $\epsilon$  improves obesity-related metabolic dysfunctions in mice. *Nat Med* 19: 313-321.

Rodriguez-Roisin R, Rabe KF, Vestbo J, Vogelmeier C, Agusti A, *et al.* (2017). Global Initiative for Chronic Obstructive Lung Disease (GOLD) 20th Anniversary: a brief history of time. *Eur Respir J* 50.

Rulifson IC, Karnik SK, Heiser PW, ten Berge D, Chen H, Gu X, *et al.* (2007). Wnt signaling regulates pancreatic beta cell proliferation. *Proc Natl Acad Sci U S A* 104: 6247-6252.

Salvi SS, & Barnes PJ (2009). Chronic obstructive pulmonary disease in non-smokers. *Lancet* 374: 733-743.

Schindelin J, Arganda-Carreras I, Frise E, Kaynig V, Longair M, Pietzsch T, *et al.* (2012). Fiji: an open-source platform for biological-image analysis. *Nat Methods* 9: 676-682.

Schindelin J, Rueden CT, Hiner MC, & Eliceiri KW (2015). The ImageJ ecosystem: An open platform for biomedical image analysis. *Mol Reprod Dev* 82: 518-529.

Schittny JC (2017). Development of the lung. *Cell Tissue Res* 367: 427-444.

Shrine N, Guyatt AL, Erzurumluoglu AM, Jackson VE, Hobbs BD, Melbourne CA, *et al.* (2019). Author Correction: New genetic signals for lung function highlight pathways and chronic obstructive pulmonary disease associations across multiple ancestries. *Nat Genet* 51: 1067.

Siddiqui FM, & Diamond JM (2018). Lung transplantation for chronic obstructive pulmonary disease: past, present, and future directions. *Curr Opin Pulm Med* 24: 199-204.

Singh D, Agusti A, Anzueto A, Barnes PJ, Bourbeau J, Celli BR, *et al.* (2019). Global Strategy for the Diagnosis, Management, and Prevention of Chronic Obstructive Lung Disease: the GOLD science committee report 2019. *Eur Respir J* 53.

Skronska-Wasek W, Gosens R, Konigshoff M, & Baarsma HA (2018). WNT receptor signalling in lung physiology and pathology. *Pharmacol Ther* 187: 150-166.

---

Skronska-Wasek W, Mutze K, Baarsma HA, Bracke KR, Alsafadi HN, Lehmann M, *et al.* (2017). Reduced Frizzled Receptor 4 Expression Prevents WNT/beta-Catenin-driven Alveolar Lung Repair in Chronic Obstructive Pulmonary Disease. *Am J Respir Crit Care Med* 196: 172-185.

Strnad P, McElvaney NG, & Lomas DA (2020). Alpha1-Antitrypsin Deficiency. *N Engl J Med* 382: 1443-1455.

Suki B, Stamenovic D, & Hubmayr R (2011). Lung parenchymal mechanics. *Compr Physiol* 1: 1317-1351.

Terzikhan N, Verhamme KM, Hofman A, Stricker BH, Brusselle GG, & Lahousse L (2016). Prevalence and incidence of COPD in smokers and non-smokers: the Rotterdam Study. *Eur J Epidemiol* 31: 785-792.

Tran FH, & Zheng JJ (2017). Modulating the wnt signaling pathway with small molecules. *Protein Sci* 26: 650-661.

Uhl FE, Vierkotten S, Wagner DE, Burgstaller G, Costa R, Koch I, *et al.* (2015). Preclinical validation and imaging of Wnt-induced repair in human 3D lung tissue cultures. *Eur Respir J* 46: 1150-1166.

66

Wang R, Ahmed J, Wang G, Hassan I, Strulovici-Barel Y, Hackett NR, *et al.* (2011). Down-regulation of the canonical Wnt beta-catenin pathway in the airway epithelium of healthy smokers and smokers with COPD. *PLoS One* 6: e14793.

Weibel ER (2013). It Takes More than Cells to Make a Good Lung. *Am J Resp Crit Care* 187: 342-346.

Wen L, Krauss-Etschmann S, Petersen F, & Yu X (2018). Autoantibodies in Chronic Obstructive Pulmonary Disease. *Front Immunol* 9: 66.

*GLOBAL HEALTH ESTIMATES 2016 SUMMARY TABLES: GLOBAL DEATHS BY CAUSE, AGE AND SEX, 2000-2016.* [Online] Available from [https://www.who.int/healthinfo/global\\_burden\\_disease/estimates/en/](https://www.who.int/healthinfo/global_burden_disease/estimates/en/). [Accessed: 26th November 2019].

Wiese KE, Nusse R, & van Amerongen R (2018). Wnt signalling: conquering complexity. *Development* 145.

---

Wright JL, Cosio M, & Churg A (2008). Animal models of chronic obstructive pulmonary disease. *Am J Physiol Lung Cell Mol Physiol* 295: L1-15.

Yeganeh B, Mukherjee S, Moir LM, Kumawat K, Kashani HH, Bagchi RA, *et al.* (2013). Novel non-canonical TGF-beta signaling networks: emerging roles in airway smooth muscle phenotype and function. *Pulm Pharmacol Ther* 26: 50-63.

Yin Y, White AC, Huh SH, Hilton MJ, Kanazawa H, Long F, *et al.* (2008). An FGF-WNT gene regulatory network controls lung mesenchyme development. *Dev Biol* 319: 426-436.

Yu W, Yang L, Li T, & Zhang Y (2019). Cadherin Signaling in Cancer: Its Functions and Role as a Therapeutic Target. *Front Oncol* 9: 989.

Zacharias WJ, Frank DB, Zepp JA, Morley MP, Alkhaleel FA, Kong J, *et al.* (2018). Regeneration of the lung alveolus by an evolutionarily conserved epithelial progenitor. *Nature* 555: 251-255.

Zepp JA, & Morrissey EE (2019). Cellular crosstalk in the development and regeneration of the respiratory system. *Nat Rev Mol Cell Biol* 20: 551-566.

Zhan T, Ambrosi G, Wandmacher AM, Rauscher B, Betge J, Rindtorff N, *et al.* (2019). MEK inhibitors activate Wnt signalling and induce stem cell plasticity in colorectal cancer. *Nat Commun* 10: 2197.

Zhang JH, Chung TD, & Oldenburg KR (1999). A Simple Statistical Parameter for Use in Evaluation and Validation of High Throughput Screening Assays. *J Biomol Screen* 4: 67-73.

Zhao WN, Cheng C, Theriault KM, Sheridan SD, Tsai LH, & Haggarty SJ (2012). A high-throughput screen for Wnt/beta-catenin signaling pathway modulators in human iPSC-derived neural progenitors. *J Biomol Screen* 17: 1252-1263.

Zimmerman ZF, Moon RT, & Chien AJ (2012). Targeting Wnt pathways in disease. *Cold Spring Harb Perspect Biol* 4.



---

# Appendix

---



---

## Acknowledgments

My first acknowledgement is to Melanie Königshoff, my PhD supervisor, for giving me this incredible opportunity to do my PhD thesis in her lab and for making everything possible. As a woman in science and as an early career scientist, I very much value all her mentorship, dedication and encouragement during my PhD.

I am also very grateful to my PhD thesis committee members Reinoud Gosens and Hadian Kamyar for great guidance and support throughout the years.

I would like to thank the PhD programs of the Comprehensive Pneumology Center Research School Lung Biology and Disease, through Claudia Staab-Weijnitz, Hoeke Baarsma, Doreen Franke and Camille Beunèche; the Helmholtz Graduate School Environmental Health (HELENA), through Monika Beer; and the Munich Medical Research School (MMRS), through Alice Edler and Antje Hentrich, for their support and for creating amazing career development opportunities.

I am grateful to all the amazing Pink lab – Munich previous and current members and guests: Ali, Aina, Ana, Andrea, Astrid, Carlo, Cedric, Chiharu, Darcy, Florian, Franzi, Hani, Henrik, Hoeke, JP, Julia, Kathrin H., Kathrin M., Lara, Mareike, Marlene, Martina, Nadine, Noor, QJ, Rabea, Sarah, Simone, Stephan, Thanu and Viola, for all scientific input, technical support, but also friendship and good times. A special acknowledgement to Darcy Wagner for supporting my PhD projects and my personal and scientific growth. Darcy was a great mentor to me, through her example and dedication to science and never ending source of constructive criticism, rigor, creativity, persistence, motivation and kindness.

I am also grateful to the Pink lab - Denver previous and current members Chiara, Katharina, Kristi, Olivier, Ricardo and Yan. It was a valuable experience being part

---

of this successful “transatlantic team” with active discussions and intercontinental experiments. I would like to thank especially Kristi for all her support during the animal experiments for this project and for her hospitality during my visit to the US.

I would like to acknowledge everyone at the Comprehensive Pneumology Center and Helmholtz Zentrum München for their collegiality and “open doors”. Special thank you to my CPC Research School colleagues, Aina, Carol, Flávia, Martina, Nina, Raphael, Stephan and Wiola for their friendship. *Um obrigada muito especial à Flávia por toda a amizade e presença nos bons e menos bons momentos do nosso tempo como alunas de doutoramento. Nunca esquecerei o seu apoio incondicional.*

*Obrigada aos meus amigos e família, em especial ao meu Pai, Armando, irmãos, Juliana e César, e avó, Cesarina, por em tanto contribuírem para o que sou hoje, por me apoiarem em todas as minhas decisões, mesmo estando longe, por toda a confiança e por nunca duvidarem das minhas capacidades.*

“A bird sitting on a tree is never afraid of the branch breaking, because its trust is not on the branch but on its own wings” - Charlie Wardle.

*Por fim, um profundo agradecimento ao Pedro, pelo maravilhoso marido e pai que é. Esta conquista também é dele e tem outro sabor com ele ao meu lado.*

“Years may pass and times may change, but I will always be by your side.

---

# List of scientific publications

## PEER-REVIEWED RESEARCH ARTICLES

---

1. Conlon T. M.\*, John-Schuster G.\*, Heide D., Pfister D., Lehmann M., Ertüz Z., Ansari M., Strunz M., Mayr C., Angelidis I., Hu Y., Ciminieri C., **Costa R.**, Kohlheppx M. S., Guillotx A., Günes G., Jeridi A., Lopez M. A., Funky M. C., Beroshvili G., Prokosch S., Hetzer J., Verleden S. E., Alsafadi H., Lindner M., Burgstaller G., Becker L., Irmeler M., Dudekz M., Goffina E., Knollez P., Pirotea B., Stoeger T., Beckers J., Wagner D. , Singh I., Theis F., Hrabé de Angelis M., O'Connor T., Tackex F., Boutrosy M., Dejardin E., Eickelberg O., Schiller H., Königshoff M., Heikenwalder M., Yildirim A.Ö.. Inhibition of LTβR-signaling blocks epithelial apoptosis and activates Wnt-induced regeneration in lung. *Nature*, 2020.
2. Lehmann M., Hu Q., Hu Y., Hafner K., **Costa R.**, van den Berg A., Königshoff M.. Chronic WNT/β-catenin signaling induces cellular senescence in lung epithelial cells. *Cell Signalling*, 2020.
3. Altunbulakli C.\*, **Costa R.\***, Lan F.\*, Zhang N., Akdis M., Bachert C. and Akdis C. A.. *Staphylococcus aureus* enhances the tight junction barrier integrity in healthy nasal tissue, but not in nasal polyps. *Journal of Allergy and Clinical Immunology*, 2018.
4. Lehmann M., Korfei M., Mutze K., Klee S., Skronska-Wasek W., Alsafadi H.N., Ota C., **Costa R.**, Schiller H.B., Lindner M., Wagner D.E., Günther A. and Königshoff M.. Senolytic drugs target alveolar epithelial cell function and attenuate experimental lung fibrosis ex vivo. *European Respiratory Journal*, 2017.
5. Skronska-Wasek W., Mutze K., Baarsma H.A., Bracke K.R., Alsafadi H.N., Lehmann M., **Costa R.**, Stornaiuolo M., Novellino E., Brusselle G.G., Wagner D.E., Yildirim A.Ö. and Königshoff M.. Reduced Frizzled Receptor 4 Expression Prevents WNT/β-Catenin-driven Alveolar Lung Repair in Chronic Obstructive Pulmonary Disease. *American Journal of Respiratory and Critical Care Medicine*, 2017.
6. Uhl F.E., Vierkotten S., Wagner D.E., Burgstaller G., **Costa R.**, Koch I., Lindner M., Meiners S., Eickelberg O. and Königshoff M. Preclinical validation and imaging of Wnt-induced repair in human 3D lung tissue cultures. *European Respiratory Journal*, 2015.

## PEER-REVIEWED REVIEWS

---

7. Khan Mirzaei M., Xue J., **Costa R.**, Ru J., Schulz S., Taranu Z. E., Deng L.. Challenges of studying the human virome - relevant emerging technologies. *Frontiers in Microbiology*, 2020
8. Ubags N. D., Baker J., Boots A., **Costa R.**, El-Mehrie N., Fabré A., Faiz A., Greene C., Heijink I., Hiemstra P. S., Lehmann M., Meiners S., Rolandsson Enes S., Bartel S.. ERS International congress, Madrid, 2019: highlights from the Basic and Translational Science Assembly. *European Respiratory Journal Open Research*, 2020.
9. Brandsma CA., Vries M., **Costa R.**, Woldhuis R.R., Königshoff M. and Timens W.. Lung ageing and COPD: is there a role for ageing in abnormal tissue repair? *European Respiratory Review*, 2017.
10. Akdis M., Aab A., Altunbulakli C., Azkur K., **Costa R.A.**, Cramer R., Duan S., Eiwegger T., Eljaszewicz A., Ferstl R., Frei R., Garbani M., Globinska A., Hess L., Huitema C., Kubo T., Komlosi Z., Konieczna P., Kovacs N., Kucuksezer U.C., Meyer N., Morita H., Olzhausen J., O'Mahony L., Pezer M., Prati M., Rebane A., Rhyner C., Rinaldi A., Sokolowska M., Stanic B., Sugita K., Treis A., van de Veen W., Wanke K., Wawrzyniak M., Wawrzyniak P., Wirz O.F., Zakzuk J.S. and Akdis C.A.. Interleukins (from IL-1 to IL-38), interferons, transforming growth factor β, and TNF-α: Receptors, functions, and roles in diseases. *Journal of Allergy and Clinical Immunology*, 2016.

---

**PEER-REVIEWED EDITORIAL**

---

11. **Costa R.**, Königshoff M.. Linking Wnt Signaling to Mucosal Inflammation. American Journal of Respiratory Cell and Molecular Biology, 2017.

\*authors equal contribution

---

## ***Affidavit***

I hereby declare that the submitted thesis entitled “Therapeutic Wnt/ $\beta$ -catenin activation and regulation for lung repair in chronic obstructive pulmonary disease” is my own work.

I have only used the sources indicated and have not made unauthorized use of services of a third party. Where the work of others has been quoted or reproduced, the source is always given.

I further declare that the submitted thesis or parts thereof have not been presented as part of an examination degree to any other university.

Munich, 27<sup>th</sup> November 2020

vii

---

Rita Costa.



---

## **Confirmation of congruency**

I hereby declare that the electronic version of the submitted thesis, entitled “Therapeutic Wnt/ $\beta$ -catenin activation and regulation for lung repair in chronic obstructive pulmonary disease” is congruent with the printed version, both in content and format.

Munich, 27<sup>th</sup> November 2020

Rita Costa.